SEC16A is a RAB10 effector required for insulin-stimulated GLUT4 trafficking in adipocytes

Joanne Bruno,[1,3]* Alexandria Brumfield,[1]* Natasha Chaudhary,[1] David Iaea,[1] and Timothy E. McGraw[1,2]

[1]Department of Biochemistry and [2]Department of Cardiothoracic Surgery, Weill Cornell Medical College, New York, NY 10065
[3]Weill Cornell/Rockefeller/Sloan Kettering Tri-Institutional MD-PhD Program, New York, NY 10065

RAB10 is a regulator of insulin-stimulated translocation of the GLUT4 glucose transporter to the plasma membrane (PM) of adipocytes, which is essential for whole-body glucose homeostasis. We establish SEC16A as a novel RAB10 effector in this process. Colocalization of SEC16A with RAB10 is augmented by insulin stimulation, and SEC16A knockdown attenuates insulin-induced GLUT4 translocation, phenocopying RAB10 knockdown. We show that SEC16A and RAB10 promote insulin-stimulated mobilization of GLUT4 from a perinuclear recycling endosome/TGN compartment. We propose RAB10–SEC16A functions to accelerate formation of the vesicles that ferry GLUT4 to the PM during insulin stimulation. Because GLUT4 continually cycles between the PM and intracellular compartments, the maintenance of elevated cell-surface GLUT4 in the presence of insulin requires accelerated biogenesis of the specialized GLUT4 transport vesicles. The function of SEC16A in GLUT4 trafficking is independent of its previously characterized activity in ER exit site formation and therefore independent of canonical COPII-coated vesicle function. However, our data support a role for SEC23A, but not the other COPII components SEC13, SEC23B, and SEC31, in the insulin stimulation of GLUT4 trafficking, suggesting that vesicles derived from subcomplexes of COPII coat proteins have a role in the specialized trafficking of GLUT4.

Introduction

Insulin regulates whole-body glucose homeostasis in part by stimulating the uptake of glucose into muscle and adipose tissues (Leto and Saltiel, 2012). Insulin stimulates glucose uptake by acutely controlling the amount of glucose transporter 4 (GLUT4) in the plasma membrane (PM; Huang and Czech, 2007; Stöckli et al., 2011). In unstimulated fat and muscle cells, GLUT4 is actively sequestered intracellularly through rapid endocytosis and slowed recycling back to the PM. Upon insulin stimulation, GLUT4 exocytosis is accelerated and internalization is slowed, resulting in a steady-state increase of GLUT4 in the PM and a corresponding increase in glucose uptake (Martin et al., 2000a, 2006; Karylowski et al., 2004). Insulin-stimulated GLUT4 translocation to the PM of muscle and fat cells is blunted in insulin resistance and type 2 diabetes, contributing to systemic dysregulation of glucose metabolism (Abel et al., 2001; Chen et al., 2011).

GLUT4 is ferried to the PM by GLUT4-specialized vesicles (GSVs) that form from the perinuclear recycling endosome/TGN compartment in adipocytes (Leto and Saltiel, 2012). In basal adipocytes, delivery of GSVs to the PM is inefficient, and the GSVs ultimately refuse with endosomes, excluding

GLUT4 from the cell surface (Karylowski et al., 2004). Activation of the insulin receptor triggers a series of molecular events that mediate the efficient formation, delivery, docking, and fusion of GSVs to the PM (Gonzalez and McGraw, 2006; Bai et al., 2007; Xiong et al., 2010), resulting in increased GLUT4 at the cell surface. In both basal and insulin-stimulated conditions, PM GLUT4 is in equilibrium with intracellular GLUT4, and therefore, the balance of endocytosis to recycling actively maintains the amount of GLUT4 on the cell surface.

An essential aspect of insulin control of GLUT4 trafficking is inhibition of AS160/TBC1D4, a Rab GTPase-activating protein (GAP; Sano et al., 2003; Eguez et al., 2005; Larance et al., 2005). Knockdown of AS160 results in a fourfold increase of GLUT4 in the PM of basal adipocytes (Eguez et al., 2005). RAB10 is the relevant AS160 target RAB protein in adipocytes that mediates this effect. Knockdown of RAB10 in cultured adipocytes cells or knockout in primary adipocytes results in an ~50% inhibition of GLUT4 translocation to the PM in response to insulin, and overexpression of RAB10 promotes GLUT4 translocation in a dose-dependent manner, demonstrating RAB10-dependent and -independent insulin regulation of GLUT4 translocation (Sano et al., 2007; Sadacca et al., 2013;

Vazirani et al., 2016). In adipocytes, RAB10 has no role in the trafficking of noninsulin responsive cargo, such as the transferrin receptor (TR; Sano et al., 2007; Chen et al., 2012). RAB10 functions at a step before the fusion of GSVs with the PM. Total internal reflection fluorescence (TIRF) microscopy studies have demonstrated that inhibition of RAB10 function blocks insulin-stimulated accumulation of GLUT4-containing vesicles near the PM without inhibiting GLUT4 vesicle fusion with the PM (Bai et al., 2007; Sano et al., 2007; Sadacca et al., 2013).

Identification of the RAB10 effectors involved in GLUT4 trafficking will provide novel insights into the adipocyte response to insulin. To this end, we used affinity chromatography to identify SEC16A as a novel RAB10 effector. We find that SEC16A and GLUT4 are localized to the perinuclear region of the cell with SEC16A concentrated around the perinuclear recycling endosome/TGN compartment containing GLUT4. SEC16A and RAB10 function in insulin-stimulated mobilization of GLUT4 from this compartment, consistent with the RAB10-SEC16A module promoting the formation of GSVs that ferry GLUT4 to the PM. The role of SEC16A in GLUT4 trafficking is independent of its previously characterized role in ER exit site function, because knockdown of other components of the ER exit site machinery, including SEC13, LRRK2, SEC23B, and SEC31, does not affect GLUT4 trafficking. However, knockdown of SEC23A, a component of COPII vesicles, blunted insulin-stimulated GLUT4 translocation but did not affect transport from the ER. These data suggest that a subcomplex of COPII coat proteins are involved in the regulated formation of GSVs that traffic GLUT4 to the PM.

Results

SEC16A is a RAB10-binding partner that regulates GLUT4 trafficking in adipocytes

To further explore the role of RAB10 in GLUT4 trafficking, we identified RAB10-GTP–binding proteins by passing lysates from insulin-stimulated 3T3-L1 adipocytes over a column of C-terminal His-tagged RAB10 loaded with GTP-γ-S. After extensive washing, RAB10 and its bound proteins were eluted from the column. Proteins in the elution fraction were identified by mass spectrometry. We focused on six eluted proteins that might be expected to have roles in membrane trafficking: IQGAP1 (IQ motif–containing GAP), ARHGEF7 (RHO GEF 7), GIT1 (an ARF GAP), PFN1 (profilin), ANXA2 (annexin 2), and SEC16A (component of ER exit sites; Table 1). We determined the effects of transiently knocking-down these proteins on insulin response. A 50% or greater knockdown, measured by quantitative RT-PCR, was achieved for each protein (Fig. S1). Only knockdown of SEC16A caused a significant blunting of

GLUT4 translocation (Fig. 1, A and B). The effect of SEC16A knockdown was rescued by reexpression of an SEC16A resistant to the siRNA, confirming the effect was caused by depletion of SEC16A (Fig. 1 C).

We determined an ~50% knockdown of SEC16A based on the cell population mean in the reduction of SEC16A mRNA, whereas we analyzed the effect of the knockdown on GLUT4 translocation at the single-cell level. To assess the relationship between the amount of SEC16A depletion and GLUT4 translocation at the cellular level, we correlated the relative expression of SEC16A in individual cells, measured by quantitative indirect immunofluorescence, to the magnitude of insulin-stimulated GLUT4 translocation. SEC16A siRNA-treated cells were binned into quartiles based on residual SEC16A expression, revealing a graded effect of SEC16A depletion that correlated with an increased inhibition of GLUT4 translocation (Fig. 1, D and E). Representative cells of the lowest and highest quartile expression of SEC16A illustrate the decreased GLUT4 translocation in cells most deplete of SEC16A (Fig. 1 F).

Although SEC16A knockdown had a significant effect on the amount of GLUT4 in the PM of insulin-stimulated adipocytes, SEC16A knockdown did not grossly alter the morphology of the intracellular GLUT4-containing compartments revealed by the GFP fluorescence of the HA-GLUT4-GFP (Fig. 1 G). As is the case in control adipocytes, GLUT4 was distributed between perinuclear compartments and dispersed punctate structures in both basal and insulin-stimulated SEC16A knockdown adipocytes. The perinuclear accumulation of GLUT4 is poorly defined, but previous studies suggest it is an element of the recycling endosomal/TGN compartment (Martin et al., 2000b; Zeigerer et al., 2002; Shi and Kandror, 2005; Huang et al., 2013). Past microscopy studies have used syntaxin 6 as a marker of this compartment, and functional studies have shown a requirement for syntaxin-6 in GLUT4 trafficking to the perinuclear site (Perera et al., 2003; Foley and Klip, 2014). In either basal or insulin-stimulated adipocytes, SEC16A knockdown did not affect targeting of GLUT4 to this syntaxin 6–positive perinuclear compartment, confirming that SEC16A affects the translocation of GLUT4 without grossly altering the intracellular itinerary of GLUT4 (Fig. 1 G).

SEC16A knockdown did not affect insulin-stimulated AKT and AS160 phosphorylation, two components upstream of RAB10 in the insulin signal transduction cascade, demonstrating that the effect of SEC16A knockdown is not secondary to a blunting of insulin signaling (Fig. 2 A).

Knockdown of RAB10 in adipocytes does not affect TR trafficking (Sano et al., 2007; Sadacca et al., 2013). As expected of a RAB10 effector, SEC16A depletion did not alter the amount of TR in the PM of basal or insulin-stimulated adipocytes when analyzed as a population mean or by quartile of SEC16A

Table 1. **RAB10-interacting proteins identified by mass spectrometry**

Gene name	Protein	Annotated function[a]
PFN1	Profilin	Actin-binding protein
ANXA2	Annexin 2	Ca-dependent phospholipid-binding protein
GIT1	G protein–coupled receptor kinase–interacting protein	ARF GAP
SEC16A	SEC16 homologue	COPII vesicle transport/ER exit sites
IQGAP1	IQ motif–containing GAP	Cell morphology and signaling
ARHGEF7	RHO GEF 7	RHO activation

[a]As annotated in Genecards (http://www.genecards.org/).
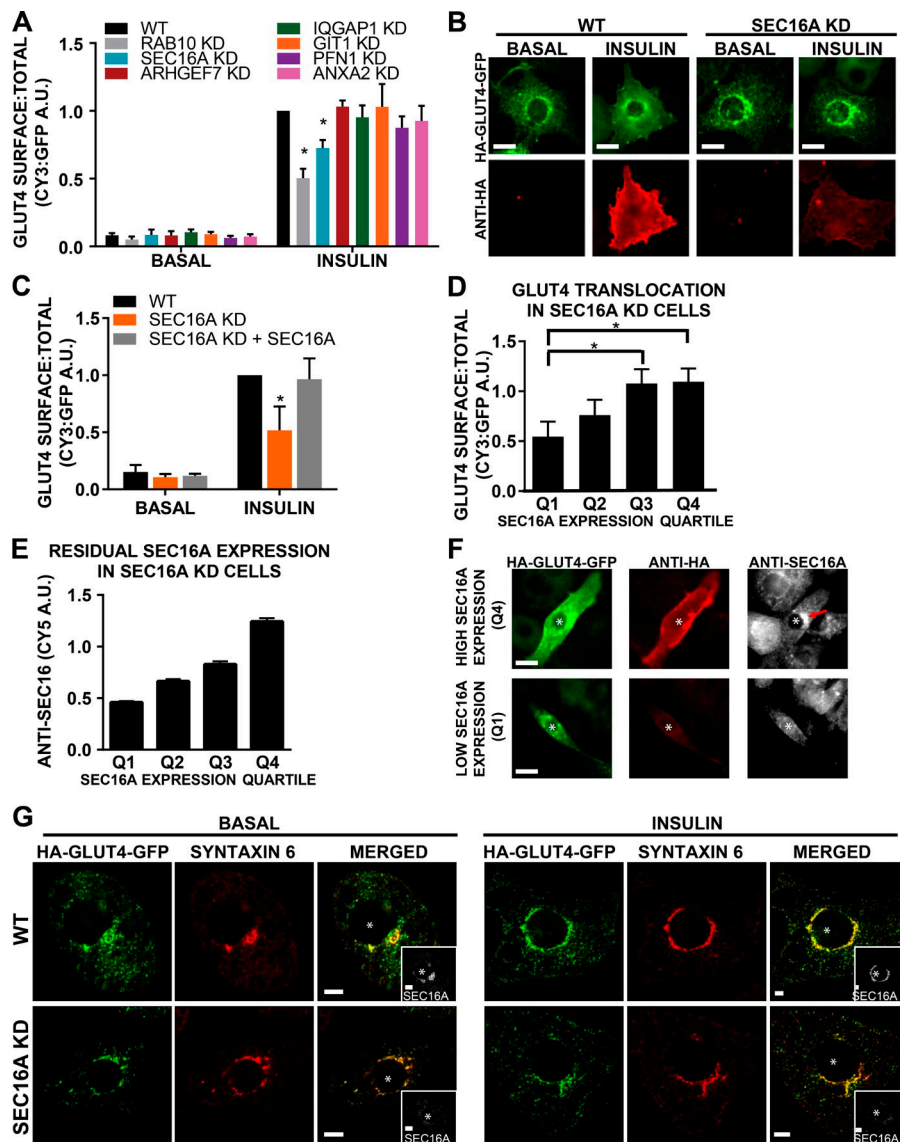
Figure 1. **SEC16A is required for GLUT4 translocation.** (A) Quantification of PM to total HA-GLUT4-GFP in adipocytes transfected with siRNA targeting the noted proteins. More than 20 cells quantified per condition per assay. Mean normalized values ± SEM. (B) Epifluorescence images of HA-GLUT4-GFP in basal and 1 nM of insulin-stimulated control and SEC16A knockdown adipocytes. Total expression of HA-GLUT4-GFP is revealed by the GFP fluorescence, and PM is revealed by immunofluorescence (IF) against HA epitope in fixed, nonpermeabilized cells. (C) Quantification of PM (surface) to total HA-GLUT4-GFP in SEC16A knockdown adipocytes with or without SEC16A cDNA. Mean normalized values ± SEM. (D) SEC16A knockdown cells are binned into quartiles based on the integrated residual SEC16A expression (x axis) determined by IF of endogenous SEC16A. The mean GLUT4 surface-to-total of cells in each quartile ± SEM, normalized to the WT population mean GLUT4 surface-to-total, is plotted (y-axis). 40 cells analyzed/assay. (E) SEC16A knockdown cells binned into quartiles based on residual SEC16A expression (x axis). Shown is the mean integrated anti-SEC16A (Cy5 fluorescence) intensity of cells in each quartile ± SEM, normalized to the control population mean anti-SEC16A intensity (y axis). 40 cells were analyzed in each assay. (F) Representative epifluorescence images from D and E of HA-GLUT4-GFP–expressing cells with the highest (Q4) and lowest (Q1) expression of SEC16A. Total HA-GLUT4-GFP is revealed by the GFP fluorescence and PM by IF against the HA epitope in fixed, nonpermeabilized cells. Endogenous SEC16A revealed by IF. Red arrow notes high expression of perinuclear SEC16A. In contrast, low-expressing cells lack this perinuclear accumulation of SEC16A while maintaining diffuse background anti-SEC16A staining. (G) Representative Airyscan confocal single-plane images of HA-GLUT4-GFP–expressing control and SEC16A knockdown adipocytes in the basal and 1 nM insulin-stimulated conditions. Endogenous synatxin-6 (Cy3) revealed by IF. Bars, 5 µm. Asterisks indicate nuclei. A.U., arbitrary units; KD, knockdown; WT, wild type. *, P < 0.05, compared to WT unless otherwise indicated.

remaining in the knockdown cells (Fig. 2, B and C). Thus, the effect of SEC16A depletion on GLUT4 trafficking is not secondary to a perturbation in general membrane trafficking.

SEC16A knockdown inhibition of GLUT4 translocation is not secondary to ER exit site dysfunction

SEC16A has a role in the export of proteins from the ER (Hughes et al., 2009; Miller and Barlowe, 2010). SEC16A acts to nucleate the formation of COPII vesicles (Watson et al., 2006; Bhattacharyya and Glick, 2007; Iinuma et al., 2007; Whittle and Schwartz, 2010; Cho et al., 2014; Sprangers and Rabouille, 2015).

To investigate if the defect in GLUT4 translocation upon SEC16A depletion was secondary to dysregulation of the exit of proteins from the ER, we determined the effects of knockdown of proteins involved in the formation of COPII vesicles on GLUT4 translocation: SEC13, which interacts with SEC16A on the ER membrane to define sites of COPII coat formation;

leucine-rich repeat kinase 2 (LRRK2), which has a role in recruiting SEC16A to the ER membrane; SEC31, which has a role in cargo selection and vesicle formation; and SEC23A and SEC23B, COPII coat proteins (Hughes et al., 2009; Whittle and Schwartz, 2010; Cho et al., 2014). Knockdowns were confirmed by RT-PCR (Fig. S1). Depletion of SEC23B, SEC13, SEC31, or LRRK2 had no effect of insulin-stimulated GLUT4 translocation, suggesting that the blunting of GLUT4 translocation in SEC16A KD adipocytes was not secondary to ER exit site dysregulation (Fig. 3 A). However, knockdown of SEC23A had a significant inhibitory effect on insulin-stimulated GLUT4 translocation (Fig. 3 A). This effect was not secondary to alterations in endosomal membrane trafficking because TR trafficking was not affected by SEC23A knockdown (Fig. 3 B). Thus, only two of the components of the machinery that regulates ER traffic tested, SEC16A and SEC23A, impact GLUT4 trafficking.

To further explore the link between ER exit and GLUT4 translocation, we quantified the effects of knockdowns on secretion of adipsin, an adipocyte-secreted protein that traffics to the
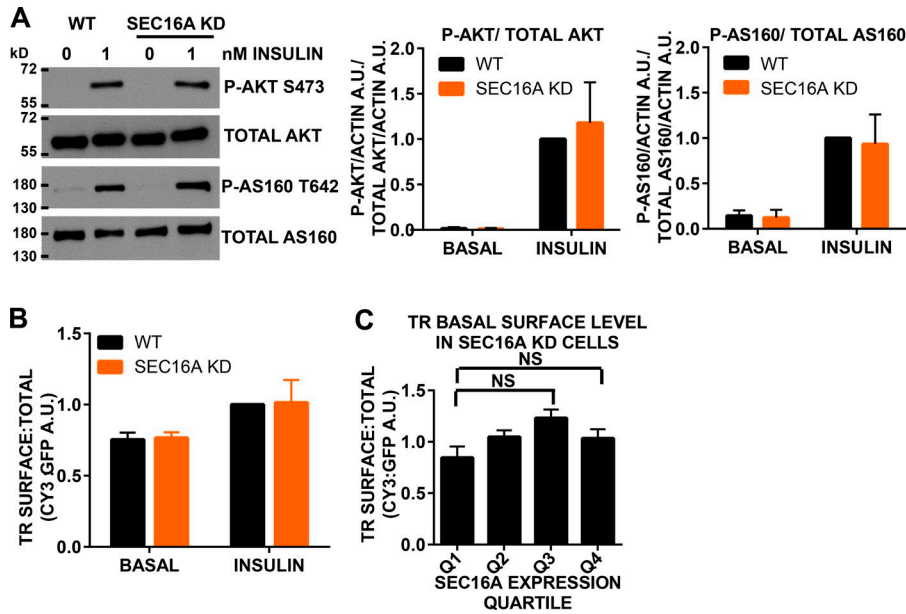
Figure 2. **SEC16A KD does not affect insulin signal transduction or TR trafficking.** (A) Western blot and corresponding densitometry quantification of AKT and AS160 phosphorylation in response to 1 nM of insulin treatment in control and SEC16A knockdown adipocytes. (B) Quantification of PM to total transferrin receptor (TR) in control and in SEC16A knockdown adipocytes. Data are normalized to the TR surface-to-total value for control adipocytes with 1 nM insulin treatment for each experiment. 40 cells were analyzed per assay. Mean normalized values ± SEM. (C) SEC16A knockdown cells are binned into quartiles based on the integrated residual SEC16A expression (x axis). The mean TR surface-to-total of cells in each quartile, normalized to the control population mean TR surface-to-total (y axis). 120 cells were analyzed. Data are from a representative experiment. Means ± SEM. In all panels, $n = 3$–5 assays; *, $P < 0.05$, compared with control unless otherwise indicated. A.U., arbitrary units; KD, knockdown; NS, not significant; WT, wild type.

PM in vesicles other than GLUT4 (Millar et al., 2000). To synchronize exit from the ER, we incubated cells in Brefeldin A for 45 min to block exit from the ER and collected media after treatment at intervals out to 3 h. We determined the amount of adipsin in the media and associated with cells by quantitative Western blotting (Fig. 3, C and D). Knockdown of SEC16A or SEC13 significantly reduced adipsin secretion, confirming a role for these proteins in ER exit. The fact that knockdowns of SEC16A and SEC13 inhibit secretion to the same extent, but only SEC16A has an effect on insulin-stimulated GLUT4 translocation, establishes that the effect of SEC16A knockdown is not secondary to an effect of ER exit. SEC23A knockdown did not affect adipsin secretion (Fig. 3, C and D; and Fig. S2). Thus, in adipocytes, SEC23A is required for GLUT4 translocation, but not for ER exit.

RAB10 does not regulate the ER pool of SEC16A

RAB10 is localized to dynamic tips of reticular ER in proliferative COS-7 cells, functioning in the maintenance of ER dynamics (English and Voeltz, 2013), raising the possibility that RAB10 might have a role in ER exit in differentiated adipocytes. However, RAB10 knockdown, unlike SEC16A knockdown, did not inhibit adipsin secretion, indicating that exit from the ER in adipocytes occurs independent of RAB10 (Fig. 3, C and D). Therefore, the function of SEC16A in transport from the ER is independent of RAB10, suggesting that in differentiated adipocytes there are at least two functional pools of SEC16A: one required at the ER and the other for GLUT4 translocation.
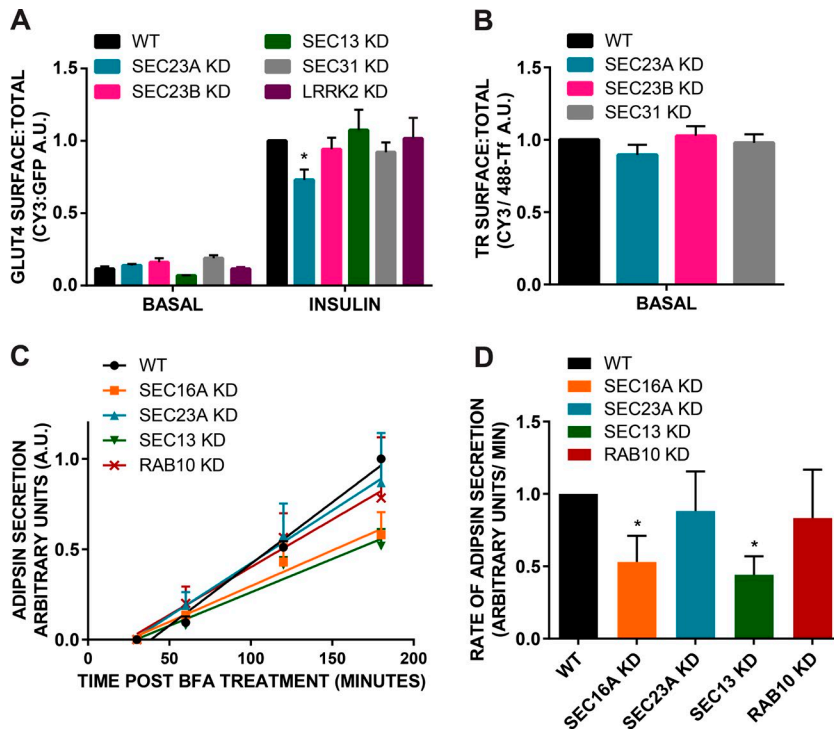
Figure 3. **SEC16A independently regulates ER-to-Golgi and GLUT4 trafficking.** (A) Quantification of surface to total HA-GLUT4-GFP in control and SEC13, SEC23A, SEC23B, SEC31, or LRRK2 knockdown adipocytes. Data normalized to the HA-GLUT4-GFP surface-to-total value for control adipocytes with 1nM insulin treatment for each experiment. (B) Quantification of PM to total TR distribution in control and SEC23A, SEC23B, or SEC31 knockdown adipocytes. Data normalized to the basal TR surface-to-total value for WT adipocytes. (C) Quantification of relative adipsin secretion at indicated time points after Brefeldin A treatment in control and SEC16A, SEC23A, SEC13, or RAB10 knockdown adipocytes. Data for individual experiments have been normalized to the wild-type 180-min value. Mean normalized values from three to four assays ± SEM, with a linear fit applied, are displayed. (D) Mean rate of adipsin secretion calculated from a linear fit of the data in Fig. 2 C. Mean normalized values ± SEM, $n = 3$–4 assays; *, $P < 0.05$, compared with WT. A.U., arbitrary units; KD, knockdown; WT, wild type.
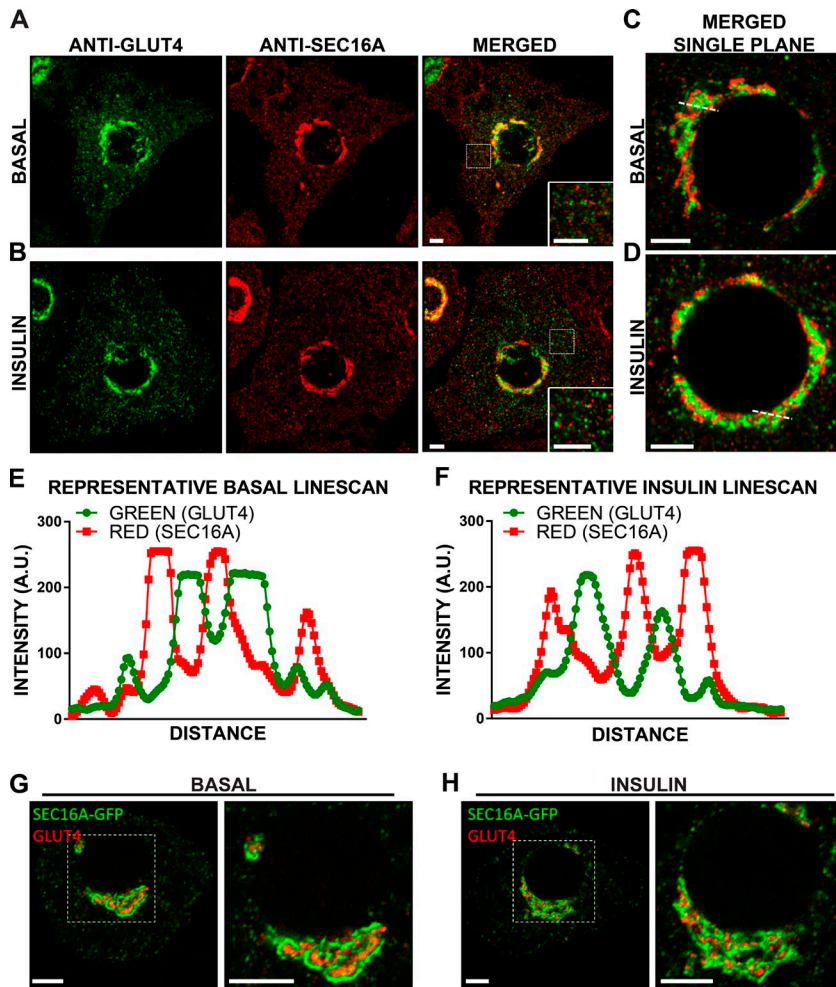
Figure 4. **SEC16A encircles perinuclear GLUT4 in adipocytes.** (A and B) Representative Airyscan confocal projections of endogenous GLUT4 (green) and endogenous SEC16A (red) in basal (A) and 1 nM of insulin-stimulated adipocytes (B). Endogenous GLUT4 and SEC16A are revealed by IF. Boxed regions magnified in insets illustrates lack of colocalization between GLUT4 and SEC16A in cytosolic puncta. (C and D) Single-plane images, taken from the middle of collected z-stacks, focused on perinuclear region of cells shown in A and B. (E and F) Line-scan quantifications for the indicated lines drawn across the perinuclear region in C and D illustrates that SEC16A tubules are adjacent to perinuclear GLUT4 compartments in basal (E) and insulin-stimulated adipocytes (F). (G and H) Representative Airyscan confocal single plane images of endogenous GLUT4 (Cy3) and transiently expressed SEC16A-GFP in basal (G) and 1 nM of insulin-stimulated adipocytes (H). Endogenous GLUT4 is revealed by IF. Bars, 5 μm. A.U., arbitrary units.

SEC16A encircles the perinuclear endosomal/TGN GLUT4 compartment

We used ZEISS airy scanning confocal microscopy (lateral resolution of ~140 nm) to investigate the colocalization of endogenous GLUT4 and endogenous SEC16A. These proteins are located together in the perinuclear region of adipocytes, with no localization in vesicles (puncta) distributed throughout the cytosol (Fig. 4 A). In the perinuclear region, SEC16A was in linear structures abutting GLUT4-containing membranes, and insulin stimulation did not affect the morphology of either the SEC16A or GLUT4 compartments (Fig. 4, A–D). SEC16A labeling defined the "edges" of the GLUT4-containing compartments, although line-scan analyses demonstrated that SEC16A does not colocalize to the same pixels as GLUT4 (Fig. 4, E and F; and Fig. S3).

Ectopically expressed SEC16A-GFP had a distribution identical to that of endogenous SEC16A, encircling the perinuclear accumulation of GLUT4 in basal and insulin-stimulated adipocytes, validating the use of this construct as a reporter for endogenous SEC16A (Fig. 4, G and H).

Perinuclear SEC16A does not colocalize with the ER

To determine whether SEC16A-labeled linear structures adjacent to the GLUT4 are SEC16A bound to the surface of ER tubules, we compared the localization of endogenous SEC16A and GLUT4 to the ER labeled by expression of SEC61B-GFP (Fig. 5 and Fig. S4). The linear SEC16A staining in the peri-

nuclear region did not significantly overlap with tubular ER in either basal or insulin-stimulated cells, suggesting these structure are not ER tubules. Furthermore, there was no overlap or obvious relationship between ER structures and the perinuclear tubular accumulation of GLUT4.

SEC16A knockdown does not alter ER morphology

Endosomes form contact sites with the ER that are spatially and temporally linked to vesicle fission (Rowland et al., 2014). Thus, the effect of SEC16A knockdown on GLUT4 translocation might be driven by changes in ER morphology (i.e., reduced reticular ER). To address this possibility, we examined the effect of SEC16A knockdown on the morphology of the ER assessed by SEC61B-GFP (Fig. 6, A and B). SEC16A knockdown did not grossly affect SEC61B-GFP morphology in either basal or insulin-stimulated cells. These data establish that the effect of SEC16A knockdown on GLUT4 was not secondary to a pronounced change in ER reticular morphology.

RAB10 and SEC16A interact in situ

We used an in situ proximity ligation assay (PLA) to probe the proximity of RAB10 and SEC16A in intact adipocytes. This microscopy-based technique detects the proximity of two antibodies within 40 nm of one another (Söderberg et al., 2006). Because the available anti-RAB10 antibodies do not work in immunofluorescence, we cotransfected adipocytes with FLAG-

A BASAL

SEC61B-GFP | SEC16A | SEC61B-GFP SEC16A
SEC61B-GFP | GLUT4 | SEC61B-GFP GLUT4
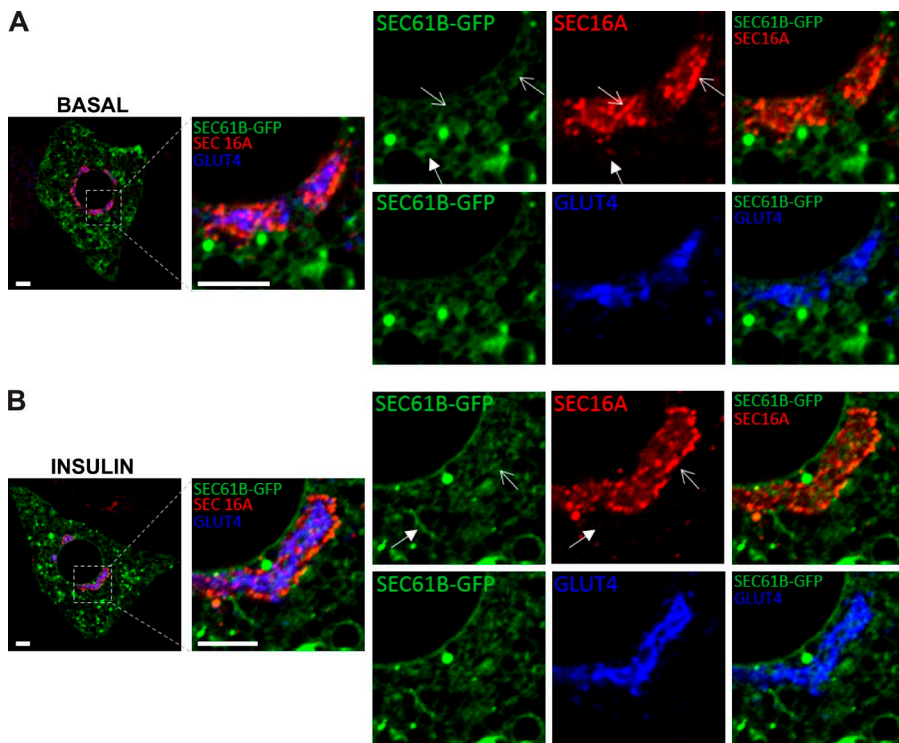
Figure 5. **The ER marker SEC61B-GFP does not colocalize with perinuclear SEC16A or surround perinuclear GLUT4.** (A and B) Representative Airyscan confocal single plane images of basal (A) and insulin-stimulated adipocytes (B) transiently expressing SEC61B-GFP. Endogenous GLUT4 (Cy5) and SEC16A (Cy3) revealed by IF. Boxed regions magnified in insets illustrate individual staining for SEC61B, GLUT4, and SEC16A. Solid arrowheads denote tubules labeled with SEC61B-GFP that are not positive for SEC16A, and arrows denote tubules labeled with SEC16A that are not positive for SEC61B-GFP. Bars, 5 µm.

B INSULIN

SEC61B-GFP | SEC16A | SEC61B-GFP SEC16A
SEC61B-GFP | GLUT4 | SEC61B-GFP GLUT4

RAB10 and GFP-SEC16A and used anti-FLAG and anti-GFP antibodies for in situ PLA. More than 90% of the transiently transfected cells expressed both GFP-SEC16A and FLAG-RAB10. Thus, we restricted our analysis of the in situ PLA signal to GFP-positive cells. Cells on the same coverslips that did not express GFP were used as controls for nonspecific in situ PLA signal.

The in situ PLA signal in unstimulated adipocytes expressing GFP-SEC16A was twice that measured in cells that did not express GFP, demonstrating proximity of SEC16A and RAB10 in the absence of insulin stimulation (Fig. 7, A–C). The in situ PLA signal in basal adipocytes overlapped with, but was not restricted to, the perinuclear accumulation of SEC16A-GFP. Insulin treatment increased both the overall PLA signal (Fig. 7 B) and the overlap of the in situ PLA signal with the perinuclear SEC16A-GFP signal (Fig. 7 C). These results

demonstrate that the proximity of SEC16A and RAB10, predominantly in the perinuclear region, is enhanced by insulin, consistent with SEC16A acting as an effector of RAB10. There was no in situ PLA signal in cells cotransfected with empty GFP vector and FLAG-RAB10, indicating that the in situ PLA signal between GFP-SEC16A and FLAG-RAB10 specifically reflected proximity between the tagged proteins (Fig. 7 D).

SEC16A depletion phenocopies RAB10 depletion

Knockdown of AS160, the RAB10 GAP, results in an increase of GLUT4 in the PM of basal adipocytes because of an increase in RAB10-GTP (Sano et al., 2007). The increase in PM GLUT4 in AS160 knockdown adipocytes is rescued by RAB10 knockdown, consistent with RAB10 being the appropriate target of AS160 in adipocytes (Fig. 7 E; Sano

A SEC61B-GFP - WT **C** SEC61B-GFP - SEC16A KD
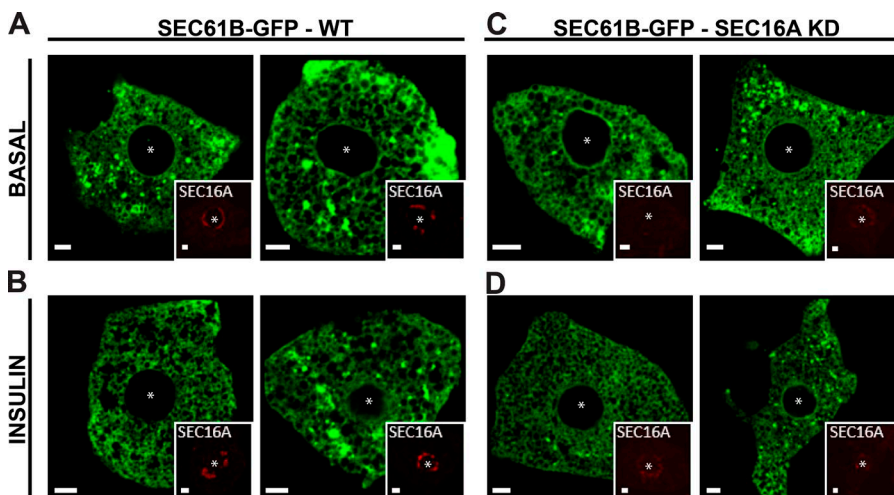
BASAL

INSULIN

Figure 6. **SEC16A is not required for maintenance of reticular ER morphology.** Representative Airyscan confocal single plane images of SEC61B-GFP transiently expressed in basal and insulin-stimulated control adipocytes (A and B) and SEC16A knockdown adipocytes (C and D). Endogenous SEC16A revealed by indirect immunofluorescence, depicted in the inset. Bars, 5 µm. Asterisks indicate nuclei. KD, knockdown; WT, wild type.
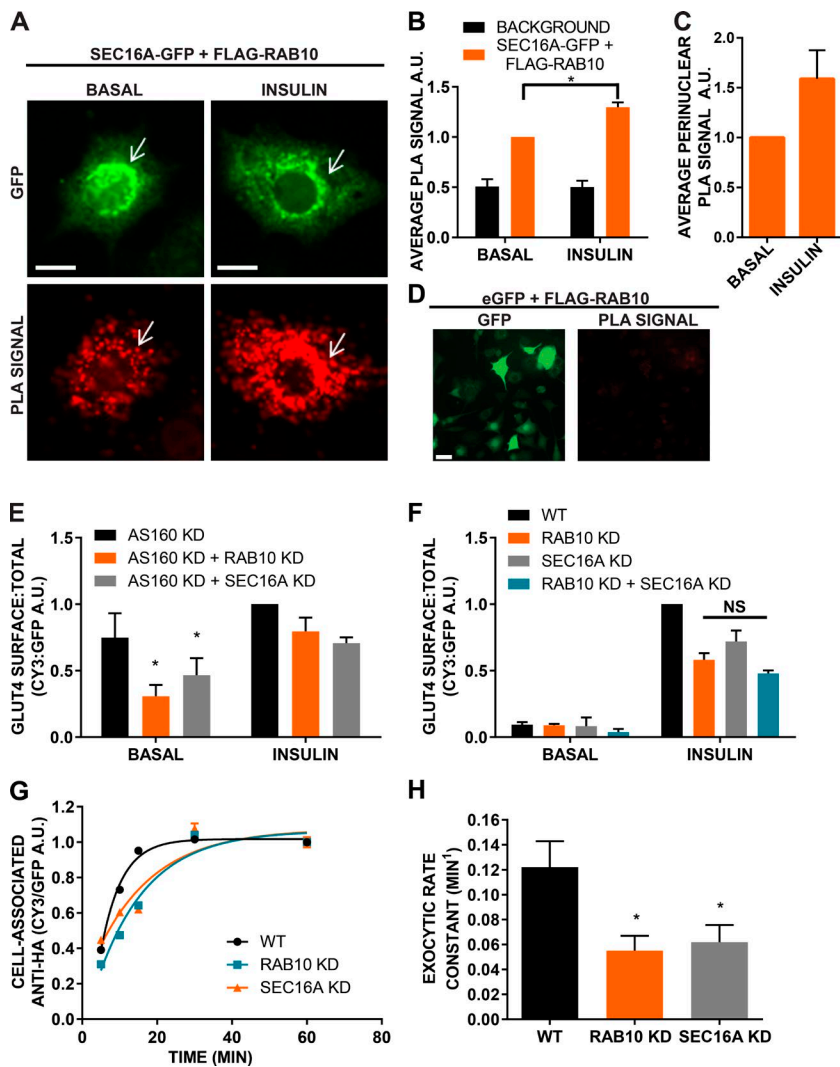
Figure 7. **SEC16A is a RAB10 effector.** (A) Representative images of in situ PLA assay performed in SEC16A-GFP and FLAG-RAB10 coexpressing adipocytes in basal and 1 nM insulin-stimulated treatment. Arrows denote SEC16A-GFP and corresponding PLA signal in the perinuclear region. Bars, 5 µm. (B) Quantification of in situ PLA signal (whole cell) shown in A. Data normalized to PLA signal in basal treatment. Mean normalized values ± SEM. (C) Quantification of in situ PLA signal from perinuclear region of cells, shown in A. Mean normalized background subtracted values ± SEM, P = 0.06 (one-tailed Student's t test). (D) Representative GFP and in situ PLA signal images of cells cotransfected with pEGFP empty vector and FLAG-RAB10 demonstrate negative controls used in experiments. Bar, 10 µm. (E) Quantification of PM to total HA-GLUT4-GFP in adipocytes in which AS160 is stably knocked down and in SEC16A or RAB10 knockdown adipocytes. (F) Quantification of PM to total HA-GLUT4-GFP in control and adipocytes in which RAB10 and SEC16A are knocked down either individually or together. (G) HA-GLUT4-GFP exocytosis in control and RAB10 or SEC16A knockdown adipocytes. Data are cell-associated anti-HA as a function of incubation time at 37°C in medium containing anti-HA antibody. Data are normalized to the 60-min time point for each condition. Mean normalized values ± SEM are shown for a representative experiment. (H) Mean exocytic rate constants determined from assays illustrated in G. Mean normalized values ± SEM, n = 3–6 assays; *, P < 0.05, compared with control. A.U., arbitrary units; eGFP, enhanced GFP; KD, knockdown; NS, not significant; WT, wild type.

et al., 2007). If SEC16A is a RAB10 effector required for GLUT4 translocation, then knockdown of SEC16A will rescue the increased GLUT4 in the PM of AS160 knockdown by functionally mitigating the effects of an increased pool of active RAB10. Knockdown of SEC16A rescued the increase in insulin-independent GLUT4 redistribution to the PM in AS160 knockdown cells, consistent with SEC16A functioning downstream of RAB10 (Fig. 7 E). There was no additive effect of simultaneously knocking down both SEC16A and RAB10 compared with either of the single knockdowns alone (Fig. 7 F), indicating that they function in the same pathway to regulate GLUT4 trafficking. Additionally, there was no compensation for the knockdown of SEC16A via changes in either RAB10 or AS160 at the protein level (Fig. S5).

RAB10 knockdown blunts the insulin stimulated increase in GLUT4 exocytosis (Sano et al., 2007). As expected of the RAB10 effector mediating insulin control of GLUT4 trafficking, knockdown of SEC16A reduced the exocytosis rate of GLUT4 in insulin-stimulated adipocytes to a similar degree as RAB10 knockdown (Fig. 7, G and H). Collectively, these data suggest that SEC16A acts downstream of RAB10 to mediate the effects of insulin on GLUT4 trafficking.

SEC16A does not colocalize with GLUT4 in vesicles beneath the PM

Past work has shown that RAB10 functions to increase GLUT4 in the PM at a step before fusion of the GLUT4-containing vesicles with the PM (Bai et al., 2007; Sano et al., 2007; Sadacca et al., 2013). The prevailing view has been that RAB10 functions to regulate GSV docking to the PM. In TIRF microscopy, imaging proteins within ∼150 nm of the PM, there is little colocalization of GLUT4 and SEC16A in either insulin-stimulated or unstimulated adipocytes, demonstrating that SEC16A is not a component of the GSVs that ferry GLUT4 to the PM (Fig. 8, A and B).

Insulin stimulation does not recruit SEC16A to the PM

The effect of insulin to increase GLUT4 to the PM is reflected by an increase of GLUT4 within the TIRF zone (Fig. 8 A). Insulin stimulation did not increase SEC16A at the PM when measured as the integrated intensity of anti-SEC16A fluorescence in TIRF microscopy or by the density of SEC16A puncta in the TIRF zone (Fig. 8, C and D). These data indicate that insulin signaling does not recruit SEC16A to the PM.

A

| HA-GLUT4-GFP TIRF | ANTI-SEC16A TIRF | MERGED |
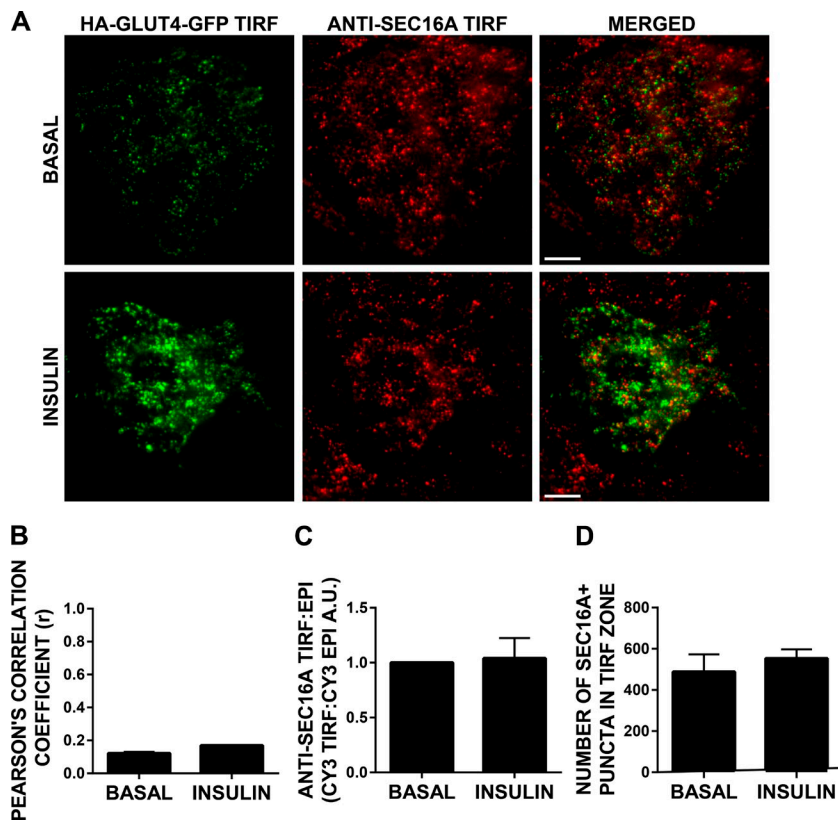
BASAL

INSULIN

Figure 8. **SEC16A does not function at the PM to regulate insulin-stimulated GLUT4 translocation.** (A) Representative TIRF microscopy images of HA-GLUT4-GFP and endogenous SEC16A (Cy3) in basal and 1 nM insulin-stimulated adipocytes. Bar, 10 μm. (B) Quantification of the colocalization of HA-GLUT4-GFP and endogenous SEC16A in TIRF microscopy. Pearson's correlation coefficient (r) is plotted for the basal and insulin-stimulated conditions. 10 cells were analyzed per condition. (C) Quantification of the integrated intensity of anti-SEC16A (Cy3) fluorescence in TIRF microscopy, normalized to the total epifluorescence intensity of anti-SEC16A (Cy3) in the cell, in basal and insulin-stimulated adipocytes (10 cells per condition). (D) Quantification of the number of SEC16A-positive puncta in TIRF microscopy in the same cells quantified in Fig. 7 C. Binary masks of SEC16A TIRF puncta above a fixed threshold were generated, and puncta with an area >2 × 2 pixels were counted (10 cells per condition). n = 2–3 assays. A.U., arbitrary units. Mean normalized value ± SEM.

SEC16A and RAB10 are required for mobilization of perinuclear endosomal/TGN GLUT4

Because we did not find SEC16A localized with GLUT4 vesicles near the PM, and because we did not find that insulin promotes the localization of SEC16A to the PM, we turned our attention to other potential sites of RAB10-SEC16A regulation of GLUT4 translocation. The known function of SEC16A in regulating COPII-coated vesicle formation suggested that SEC16A might act in the functionally equivalent step of the formation of the GSVs that ferry GLUT4 to the PM. Previous studies have shown that GSVs form from the perinuclear pool of endosomal/TGN GLUT4 (Martin et al., 2000a,b; Zeigerer et al., 2002; Shewan et al., 2003; Karylowski et al., 2004).

To determine if SEC16A knockdown reduced mobilization of GLUT4 from the perinuclear compartment, we used IRAP-TR, reporter of the insulin-regulated GLUT4 trafficking pathway (Subtil et al., 2000). In IRAP-TR, the cytoplasmic domain of IRAP replaces the cytoplasmic domain of human TR in IRAP-TR, conferring GLUT4-like trafficking on the chimera (Subtil et al., 2000; Jordens et al., 2010). The well-developed methods for characterizing the kinetics of TR trafficking can be applied to study IRAP-TR trafficking (Subtil et al., 2000).

Fluorescently labeled transferrin internalized by IRAP-TR accumulates in a perinuclear compartment that overlaps with perinuclear HA-GLUT4-GFP (Fig. 9 A). Apotransferrin bound to IRAP-TR is released from the cells when the IRAP-TR recycles back to the PM and is a measure of the recycling of IRAP-TR to the PM (Subtil et al., 2000). To measure the depletion of transferrin (Tf) specifically from the perinuclear compartment that colocalizes with GLUT4, we created a region of interest that encircled perinuclear GLUT4. The amount of Tf in this region decreased over time as vesicles bud and traffic

to the PM (Fig. 9 A). Mobilization of Tf from the perinuclear compartment of SEC16A knockdown cells was decreased compared with control cells, consistent with SEC16A having a role in GLUT4 mobilization from this perinuclear region (Fig. 9 B). RAB10 knockdown had a similar effect on insulin-stimulated mobilization of IRAP-TR from the perinuclear region (Fig. 9 B).

SEC16A localizes to GLUT4-containing membranes

SEC16A encircles GLUT4 in the perinuclear region of adipocytes (Fig. 4). We next determined if SEC16A copurifies with GLUT4-containing membranes. We isolated GLUT4-containing membranes from both basal and insulin-stimulated adipocytes stably expressing HA-GLUT4-GFP by detergent-free anti-GFP magnetic microbead immunoabsorption. We used two different concentrations of beads to achieve either near-complete or a 50% immunoabsorption of GLUT4. GLUT4 is in equilibrium among several different intracellular compartments (Karylowski et al., 2004). All of these compartments will be absorbed with near-complete GLUT4 immunoabsorption (high amount of beads). We reasoned that submaximal immunoabsorption would identify proteins that are specifically enriched in membranes containing the highest concentration of GLUT4, such as the perinuclear compartment. When we reduced the immunoabsorption of GLUT4 to ~50% in basal adipocytes, the co-absorption of AS160 and IRAP, two proteins known to traffic with GLUT4, were also reduced by ~50% (Fig. 9, C and D). The relative co-absorption of calnexin and syntaxin 6 with GLUT4 was decreased by 90% with reduced immunoabsorption of GLUT4, suggesting that these proteins, markers of the ER and a subdomain of the TGN, respectively, are not as enriched in GLUT4-containing membranes as AS160 and IRAP (Fig. 9, C and D). The observation that TGN46, another TGN
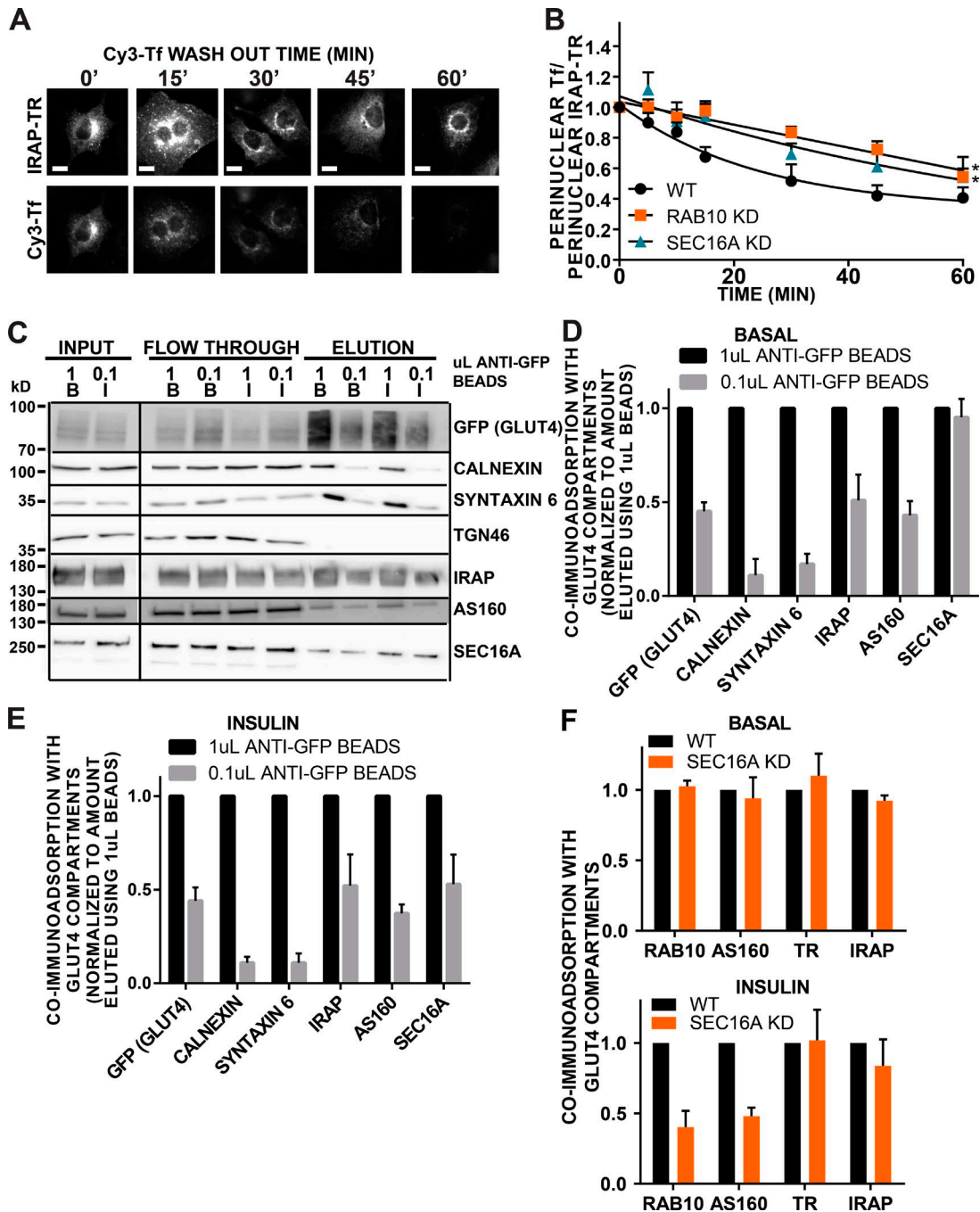
Figure 9. **SEC16A and RAB10 are required for GLUT4 vesicle mobilization from a perinuclear compartment.** (A) Representative epifluorescence images of the transferrin washout assay in adipocytes expressing IRAP-TR. Cy3-transferrin (Cy3-Tf) internalized from the medium by IRAP-TR accumulates in the perinuclear region and is released from cells upon incubation in medium without Cy3-Tf. In the top panel, detection of IRAP-TR by immunofluorescence and the corresponding Cy3-Tf images are shown below. Time is in minutes of incubation in medium without Cy3-Tf. Bars, 5 μm. (B) Quantification of Cy3-Tf washout in control adipocytes and adipocytes in which SEC16A or RAB10 were depleted by transient knockdown. Data are normalized to the perinuclear Tf/perinuclear IRAP-TR at time 0 for each experiment. *n* = 6–8 assays. Two-way analysis of variance: *, P < 0.05 compared with control. (C) Representative Western blots of immunoabsorbed HA-GLUT4-GFP compartments of basal (B) and insulin (I) stimulated adipocytes using 1 or 0.1 μl anti-GFP beads. Proteins coimmunoabsorbed with GLUT4 compartments are in the elution fraction, and proteins not coimmunoabsorbed are in the flow-through fraction. (D) Densitometry quantification of Western blots of immunoabsorbed HA-GLUT4-GFP compartments of basal (B) adipocytes shown in C. Data are coimmunoabsorption of each protein with GLUT4 compartments (band intensity in the eluted fraction) when 1 or 0.1 μl anti-GFP beads is used. For each quantification the data are normalized to the band intensity of coimmunoabsorbed protein using 1 μl beads. *n* = 3 assays. Mean normalized values ± SEM. (E) Densitometry quantification of Western blots of immunoabsorbed HA-GLUT4-GFP compartments of insulin-stimulated (I) adipocytes shown in C. Data are coimmunoabsorption of each protein with GLUT4 compartments using 1 or 0.1 μl anti-GFP bead. *n* = 3 assays. Mean normalized values ± SEM. (F) Quantification by Western blot of endogenous RAB10, AS160, TR, and IRAP coimmunoabsorbed with HA-GLUT4-GFP compartments from control and SEC16A depleted adipocytes. Mean normalized values ± SEM; *n* = 2–5 assays. KD, knockdown; WT, wild type.

marker, does not co-absorb with GLUT4-containing membranes demonstrates that GLUT4 is concentrated in a selective domain of the TGN. Interestingly, the amount of SEC16A coimmunoabsorbed with GLUT4 was not reduced, suggesting SEC16A is highly enriched with the subset of GLUT4-containing membranes that are efficiently immunoabsorbed from basal adipocytes (Fig. 9, C and D).

The results were similar for insulin-stimulated adipocytes, except for SEC16A, where there was a significant decrease in the amount of co-absorbed SEC16A in conditions of reduced GLUT4 immunoabsorption (Fig. 9, C and E). Upon insulin stimulation, GLUT4 becomes more concentrated in GSVs. SEC16A is not a component of GSVs (Jedrychowski et al., 2010), and this decrease in SEC16A association with GLUT4 compartments in insulin-stimulated cells may reflect this redistribution of GLUT4.

It is of note that there is significant SEC16A that does not co-absorb with GLUT4 (in the flow through) under conditions when >90% of GLUT4 is immunoabsorbed (Fig. 9 C). Two biochemical pools of SEC16A were expected because of the independent roles of SEC16A in regulating ER-to-Golgi trafficking, and GLUT4 mobilization from the perinuclear recycling endosome/TGN would require it to reside in these two distinct compartments.

SEC16A knockdown reduces the association of RAB10 and AS160 with GLUT4-containing membranes

If SEC16A is involved in GSV formation, then SEC16A knockdown would change the composition of GLUT4-containing vesicles. To determine if this was the case, we isolated GLUT4-containing membranes from adipocytes stably expressing HA-GLUT4-GFP by detergent-free immunoabsorption with anti-GFP magnetic microbeads (Fig. 9 E). SEC16A knockdown significantly reduced the association of AS160 and RAB10 with the GLUT4-containing compartments in insulin-stimulated cells, without an effect in the basal condition. These data provide further evidence for the role of SEC16A in AS160-RAB10 regulation of GLUT4 trafficking. Coimmunoabsorption of IRAP was unchanged by SEC16A knockdown. This was expected, because IRAP traffics by the same pathway as GLUT4, and perturbations affecting one are known to affect the other (Eguez et al., 2005; Sano et al., 2007; Jordens et al., 2010). However, TR, a marker of general endocytic trafficking, was unchanged by SEC16A knockdown in either basal or insulin-stimulated conditions, establishing that SEC16A knockdown did not result in a significant shift of GLUT4 from specialized membrane compartments to the more general Tf-positive endosomes (Fig. 9 F).

Discussion

Insulin triggers transport of blood glucose into adipocytes and muscle cells by stimulating a redistribution of GLUT4 from intracellular compartments to the PM. The amount of GLUT4 in the PM is limiting for glucose uptake, and therefore the postprandial lowering of blood glucose by disposal of glucose into adipose and muscle requires a persistent elevation of PM GLUT4 that parallels increased insulin levels. Because GLUT4 continually cycles between the PM and intracellular compartments, the maintenance of elevated cell-surface GLUT4 in the presence of insulin requires accelerated biogenesis of the
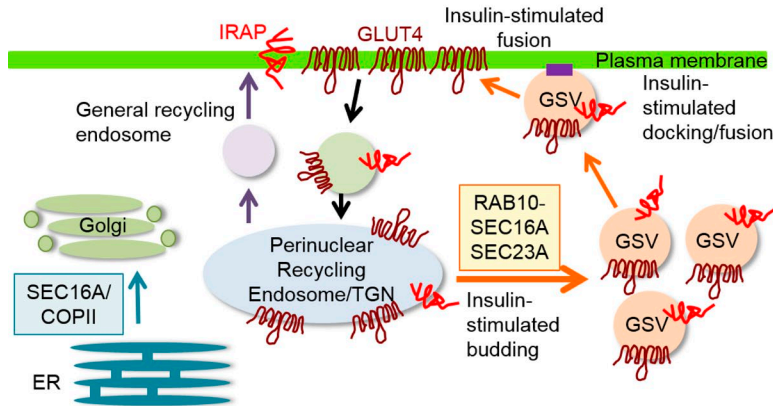
specialized vesicles that transport GLUT4 to the PM. Identifying the protein machinery that regulates GLUT4 trafficking will provide insights into the molecular mechanism underlying the control of glucose metabolism and thereby provide a framework for understanding its disruption in insulin-resistance.

Here, we establish SEC16A as a RAB10 effector involved in GLUT4 translocation. Our data support a model in which RAB10, activated downstream of insulin stimulation, interacts with SEC16A to promote the formation of the GSVs that ferry GLUT4 to the PM of adipocytes (Fig. 10). The RAB10-SEC16A module, by stimulating GSV formation, supports a persistent elevated level of GLUT4 in the PM during continued insulin stimulation. Insulin stimulation of GSV formation is impaired by knockdown of RAB10, SEC16A, or the COPII coat subunit SEC23A, resulting in a blunting of the steady-state redistribution of GLUT4 to the PM of stimulated adipocytes. Disruption of the RAB10-SEC16A module by knockdown of the individual proteins inhibits GLUT4 translocation by ~50%. This partial effect is consistent with a model in which insulin controls the amount of GLUT4 in the PM by regulating multiple trafficking steps that likely include, in addition to the stimulated formation of the GSVs via RAB10-SEC16A function, the docking and fusion of the GSVs to the PM. Recent studies support insulin control of exocyst function that contributes to GLUT4 redistribution by regulating the docking of GLUT4 vesicles to the PM (Karunanithi et al., 2014; Sano et al., 2015).

We have used several different approaches to test the hypothesis that SEC16A is an effector of RAB10 in the regulation of GLUT4 trafficking in adipocytes. First, SEC16A knockdown recapitulates the decrease in GLUT4 exocytosis seen with RAB10 knockdown, and SEC16A knockdown combined with RAB10 knockdown had no additional effect on GLUT4 translocation compared with either single knockdown. Second, both SEC16A knockdown and RAB10 knockdown restore GLUT4 retention in unstimulated AS160 knockdown adipocytes. Knockdown of AS160, a negative regulator of RAB10, results in an increase of GLUT4 in the PM in the absence of insulin stimulation, and this increase is reversed by RAB10 knockdown. SEC16A also reverses the effect of AS160 knockdown on GLUT4, which strongly supports the conclusion that SEC16A functions downstream of active RAB10. Third, similar to RAB10 knockdown, SEC16A knockdown does not affect TR trafficking or the insulin-signal transduction cascade.

It has previously been shown in TIRF microscopy studies that one effect of insulin is to promote association (tethering/docking) of GSVs with the PM (Lizunov et al., 2013) and that the AS160-RAB10 signaling module acts at a prefusion step of GLUT4 trafficking, presumably regulating the docking/tethering of GSVs to the PM (Gonzalez and McGraw, 2006; Bai et al., 2007; Sano et al., 2007; Sadacca et al., 2013). Therefore, we expected that SEC16A, as a RAB10 effector, would function at the PM. However, our data support a model in which SEC16A acts at the perinuclear recycling endosome/TGN to stimulate the formation of GSVs, thereby mobilizing insulin-regulated cargo for delivery to the PM. SEC16A is localized immediately adjacent to GLUT4 in the perinuclear compartment. There is no significant colocalization between GLUT4 and SEC16A in the TIRF zone (within 150 nm of the PM) or with GLUT4-containing vesicles distributed throughout the cytosol, demonstrating that SEC16A is not associated with GSVs, as might be anticipated if SEC16A regulated the association of these vesicles with the PM. Furthermore, insulin does not stimulate a redistribution

A Insulin-stimulated wild type cells

IRAP GLUT4 Insulin-stimulated fusion

Plasma membrane

General recycling endosome

Insulin-stimulated docking/fusion

GSV

Golgi

RAB10-SEC16A SEC23A

GSV GSV

SEC16A/COPII

Perinuclear Recycling Endosome/TGN

Insulin-stimulated budding

GSV

ER

B Insulin-stimulated RAB10 or SEC16A knockdown cells

IRAP GLUT4 Insulin-stimulated fusion

Plasma membrane

General recycling endosome

Insulin-stimulated docking/fusion

GSV

Golgi

RAB10 SEC16A SEC23A

GSV

SEC16A/COPII

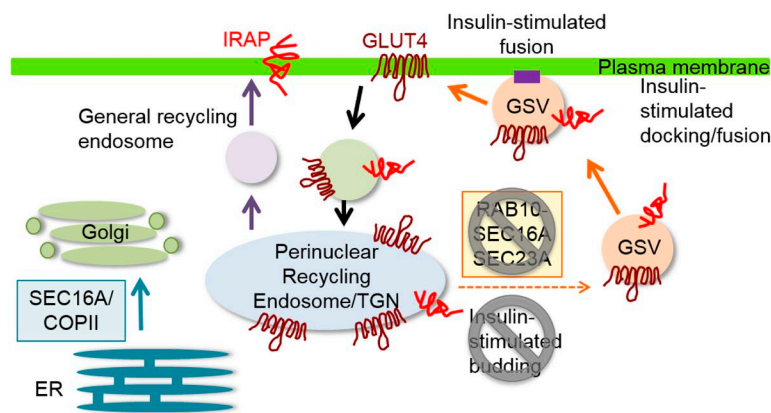Perinuclear Recycling Endosome/TGN

Insulin-stimulated budding

ER

Figure 10. **Schematic of the role of RAB10-SEC16A in insulin-regulated GLUT4 translocation.** (A) RAB10-SEC16A enhancement of GSV formation generates a constant pool of GSVs of sufficient size to maintain elevated PM GLUT4 in the presence of insulin. (B) Knockdown of RAB10 or its effector SEC16A limits the supply of GSVs, thereby blunting the insulin response. Insulin regulation of other steps of GLUT4 trafficking independent of RAB10 would support a blunted increase of GLUT4 in the PM of RAB10 or SEC16A knockdown cells.

of SEC16A to the TIRF zone, as might be expected if SEC16A regulated GSV docking in an insulin-sensitive manner. Collectively, these data are not consistent with SEC16A functioning to regulate GSV docking to the PM.

SEC16A has a role in transport from the ER by regulating the assembly of COPII vesicle components on the ER membrane (Connerly et al., 2005; Sprangers and Rabouille, 2015). Our data support RAB10-SEC16A functioning in the stimulated mobilization of GLUT4 from a perinuclear recycling endosome/TGN compartment. There are previous studies showing that insulin regulates the formation of GLUT4 vesicles, although this has not been linked to RAB10 or SEC16A (Huang et al., 2013). Our data support SEC16A acting in the biogenesis of GSVs. First, SEC16A is localized adjacent to GLUT4 in the perinuclear recycling endosome/TGN compartment, the site of GSV formation. Second, insulin increases the proximity of SEC16A and RAB10 in the perinuclear compartment (detected by in situ PLA), consistent with SEC16A acting at the perinuclear compartment of insulin-stimulated cells. Third, SEC16A or RAB10 knockdown slow the insulin-stimulated exit of IRAP-TR from the perinuclear compartment, providing direct support for RAB10-SEC16A functioning in the mobilization of cargo of the insulin-regulated pathway from the perinuclear compartment. Finally, SEC16A knockdown decreased the association of AS160 and RAB10 with GLUT4-containing membranes in insulin-stimulated adipocytes, providing support for reduced GSV formation, because both AS160 and RAB10 are components of GSVs (Jedrychowski et al., 2010). The observations that in unstimulated adipocytes neither GLUT4

trafficking nor the association of RAB10 and AS160 with GLUT4 membranes is affected by SEC16A knockdown demonstrate that SEC16A is not required for formation of GSVs in basal conditions when demand is low but is required only when the demand for GSVs is high, such as in the context of insulin stimulation. Our results do not preclude RAB10 from also acting at other prefusion trafficking steps along the GLUT4 itinerary. It has recently been reported that SEC15b, an exocyst component that interacts with RAB10 in yeast two-hybrid analyses, is also an effector of RAB10; however, the function of RAB10-SEC15b in GLUT4 trafficking has not been extensively characterized (Sano et al., 2015).

Our results establish that in differentiated adipocytes, the role of SEC16A in the ER is independent of its role in GLUT4 trafficking. Knockdown of SEC13, which functions with SEC16A to regulate exit from the ER, does not affect GLUT4 trafficking but causes the expected defect in transport from the ER. In addition, knockdown of LRRK2, a kinase that recruits SEC16A to the ER, does not inhibit GLUT4 translocation. These results uncouple general inhibition of ER exit from insulin regulation of GLUT4 trafficking. Finding SEC16A functions in both exit from the ER and GLUT4 translocation suggests there must be two functional pools of SEC16A. In agreement with this proposal, we show biochemically two pools of SEC16A in adipocytes, one that localizes to GLUT4 compartments and one that does not.

Transient knockdown of other COPII components, SEC23B and SEC31, did not blunt insulin-stimulated translocation. However, knockdown of SEC23A, another COPII

component, blunted insulin-stimulated GLUT4 translocation. Finding a subset of the COPII vesicle coat machinery components involved in GLUT4 translocation is consistent with there being functional subcomplexes of COPII components. Functional subcomplexes of the clathrin adaptor proteins and the retromer provide precedents for the possibility of functional COPII subcomplexes. In this regard, the number of paralogs of COPII components in mammalian cells makes possible a large variety of COPII coats to fulfill cargo and or tissue-specific functions (Khoriaty et al., 2012). For example, mutations in SEC23B cause congenital dyserythropoietic anemia type II, suggesting a specific role for SEC23B in erythroblasts of the bone marrow (Khoriaty et al., 2012).

SEC16A association with GLUT4 compartments is reduced by insulin stimulation, seemingly inconsistent with its proposed role in the formation of GLUT4-containing vesicles. However, during insulin stimulation, GLUT4 is mobilized from intracellular storage compartments to GSVs and SEC16A is not a component of GSVs (Jedrychowski et al., 2010), thereby explaining the decrease in SEC16A association with GLUT4-containing membranes. These results are in agreement with SEC16A function at the ER, where it has a role in generating COPII vesicles without being a component of these vesicles (Budnik and Stephens, 2009; D'Arcangelo et al., 2013).

The ER has been proposed to serve as a general platform for membrane fission and fusion events (Rowland et al., 2014). Given the role of SEC16A in ER transport, it is conceivable that the effects of SEC16A knockdown are caused by changes in ER morphology that disrupt the dynamics of membranes containing GLUT4. However, ER morphology is not altered in SEC16A knockdown cells. Furthermore, it is highly unlikely that disruption of an ER function required for general membrane fission and fusion would specifically impair GLUT4 trafficking but have no effect on general vesicular trafficking. However, SEC16A knockdown specifically inhibits GLUT4 translocation but has no effect on TR.

In addition to the role of RAB10 as a key mediator of GLUT4 trafficking in adipocytes, RAB10 functions in other cell types in the regulation of other membrane trafficking processes: sorting of recycling cargo in polarized cells (Babbey et al., 2006, 2010; Lerner et al., 2013; Deen et al., 2014; Xu et al., 2014), polarized membrane trafficking required for axon development (Habraken et al., 1999), TLR4 trafficking in macrophages (Kasprzak et al., 1998), and phagosome maturation (Penn et al., 1990). Although the specific vesicular cargo and molecular machinery required for each of these functions are quite disparate, what they have in common is that they are all regulated trafficking events in which RAB10 regulates vesicle delivery to the PM.

Recently, it was found that SEC16A functions as an integrator of growth factor signaling and secretion in HeLa cells, acting as the central node in a feed forward loop and allowing growth factors to prepare cells for the increased secretory cargo load that accompanies proliferation (Tillmann et al., 2015). Even though our data demonstrate that the effect of SEC16A knockdown on GLUT4 trafficking in adipocytes is not secondary to perturbations of flux through the ER, it is provocative to consider how SEC16A's role as a potential integrator of hormonal cues in proliferative cells has been adapted for use in terminally differentiated adipocytes, in which proliferation is not the end goal of growth factor signaling.

Materials and methods

Cell lines and culture
3T3-L1 fibroblasts were maintained in culture and differentiated into adipocytes as previously described (Zeigerer et al., 2002). For some experiments, previously described 3T3-L1 cell lines stably expressing shRNA sequences directed against RAB10 or AS160 were used (Eguez et al., 2005; Sano et al., 2007). Immunoabsorption experiments were performed using 3T3-L1 cell lines stably expressing HA-GLUT4-GFP.

DNA and siRNA constructs and quantitative PCR
The HA-GLUT4-GFP, TR, IRAP-TR, FLAG-RAB10, SEC61B-GFP, and SEC16A-GFP DNA plasmids have been described previously (Lampson et al., 2001; Bhattacharyya and Glick, 2007; Friedman et al., 2010; Jordens et al., 2010; Giordano et al., 2013; Sadacca et al., 2013). SEC16A plasmids contained sequences for human SEC16A and were resistant to knockdown by mouse SEC16A-directed siRNA sequences. For rescue experiments, we generated SEC16A-GFP in which we mutated GFP to ablate the fluorescence by the following mutations in the enhanced GFP of the SEC16A-GFP construct: T66A, Y67A, and G68A. This was done using the QuikChange II Site-Directed Mutagenesis kit (Agilent Technologies). The siRNA constructs were, wherever possible, as previously published.

Sequences were as follows: RAB10: si251, 5′-GCAUCAUGC UAGUGUAUGA-3′ (same sequence as shRNA expressed by RAB10 KD cells; Sano et al., 2007); AS160: 5′-GACTTAACTCATCCA ACGA-3′ (same sequence as shRNA expressed by AS160 knockdown cells; Eguez et al., 2005); SEC16A: si1, 5′-CTTCAGAATATC AGCTCCCTGGGGCTC-3′, si3, 5′-AGCTGGACTTGCTGGTGG CTGGGCCAA-3′; ARHGEF7: 5′-AGCAGCUUUUUCAUGUCU UGGGGCUC-3′; IQGAP1: 5′-GAGAGGAACUUGUCUGUCACG GCCCUC-3′; GIT1: 5′-GGUGGGUUAGUGUCUCGGGAGUGGCC CAG-3′; PFN1: 5′-AAAAGCCAAAGGGAACGGUGGGGGGGAA- 3′; ANXA2: 5′-AGGCCCAAAAUCACCGUCUCCAGGUGG-3′; SEC13: 5′-GGAGGCUGACACAGAACCCUGGCCCUU-3′; LRRK2: 5′-CAAGAAACUCUCAGGUCGAUUGUCUAA-3′; SEC23A: 5′- AGGUUGUCAUGGUAGCACUUGAUUCUU-3′; SEC23B: 5′-UCU GAAAGACGUAGGGUCUUCUUUGUU-3′; and SEC31: 5′-AUA UAAUACCUCUCCUGUGUUAGGGUU-3′.

When only one siRNA sequence was used, 2 nmol of that siRNA was electroporated. When two siRNAs, 2 nmol of each siRNA was electroporated. Two siRNAs targeting SEC16A were required to achieve this degree of knockdown, whereas only one was required for the other proteins. Measurement of knockdown was performed by quantitative PCR. 3T3-L1 adipocytes were electroporated with siRNAs as described. At 48 h after electroporation, cells were harvested and RNA was extracted using the RNeasy kit from QIAGEN. From extracted RNA, cDNA was made using the RNA to cDNA EcoDry Pre-mix from Takara Bio Inc., and quantitative PCR was performed using a qSTAR primer pair obtained from OriGene.

Electroporation and GLUT4 and TR translocation assays
Indicated cell lines were electroporated with 45 µg of each indicated plasmid and/or 2–4 nmol siRNA as previously described (Zeigerer et al., 2002). Assays were performed 1–2 d after electroporation, as needed to achieve knockdown of the targeted protein as validated by RT-PCR. On the day of the assay, GLUT4 or TR translocation assays were performed as described previously (Lampson et al., 2001; Zeigerer et al., 2002; Karylowski et al., 2004; Sano et al., 2007; Jordens et al., 2010). In brief, cells were washed and incubated in media without sera for 2 h. Cells were then stimulated with 1 nM insulin for 30 min to achieve steady-state surface GLUT4 levels. Cells were fixed with 3.7%

formaldehyde for 7–10 min, and an anti-HA antibody was used, without permeabilization, to label HA-GLUT4-GFP on the cell surface. HA staining was visualized with fluorescently tagged secondary antibodies, and total HA-GLUT4-GFP was visualized by direct fluorescence, as described later (Lampson et al., 2000; Karylowski et al., 2004). Mouse anti-HA was purchased from Covance, and secondary antibodies were obtained from Jackson ImmunoResearch Laboratories and Invitrogen.

For experiments where the effect of SEC16A KD on GLUT4 translocation and basal TR levels was binned into quartiles based on residual SEC16A expression, anti-HA primary and secondary staining was followed by permeabilization with 0.25 mg/ml saponin (Sigma-Aldrich) and indirect immunofluorescence with anti-mouse SEC16A antibody (MKA0310; Cosmo Bio Co.) to label endogenous SEC16A. SEC16A staining was visualized with a Cy5-labeled secondary antibody (Thermo Fisher Scientific).

For experiments assessing colocalization of endogenous SEC16A and SEC16A-GFP with endogenous GLUT4, cells were electroporated with SEC16A-GFP DNA as described, followed by permeabilization with 0.25 mg/ml saponin (Sigma-Aldrich) and indirect immunofluorescence with mouse anti-GLUT4 antibody (2213S; Cell Signaling Technology) or rabbit anti-SEC16A antibody (MKA0310; Cosmo Bio Co.) that was visualized with fluorescently tagged secondary antibody.

Microscopy, image quantification, and statistics

All epifluorescence images were collected on an inverted microscope at room temperature using a 20× air objective (Leica Biosystems) and a cooled charge-coupled device 12-bit camera. Exposure times (Jordens et al., 2010) and image quantification (Lampson et al., 2001) were performed using MetaMorph image processing software (Universal Imaging), as previously described. GFP and Cy3 fluorescence signals were background corrected and the surface(Cy3):total(GFP) (S:T) GLUT4, TR, or VSVG ratio was calculated for each cell. The S:T values were normalized within each assay to the mean S:T value for the indicated condition to allow for averaging results across multiple biological repeat assays. For experiments where SEC16A siRNA-treated cells were binned into quartiles, the integrated anti-SEC16A (Cy5) fluorescence was measured for each cell, and cells were subsequently binned into quartiles based on residual SEC16A expression. The corresponding mean GLUT4 or TR S:T value for cells in each quartile was calculated and normalized to the wild-type population mean S:T. The levels of residual SEC16A expression in each quartile was also calculated by normalizing the mean anti-SEC16A (Cy5) fluorescence of cells in each quartile to the wild-type population mean anti-SEC16A (Cy5) fluorescence. The residual SE paired Student's *t* tests were performed on raw (non-normalized) S:T mean values from multiple assays. One-tailed Student's *t* tests were only used when a reasonable expectation could be formed from previous results as to the direction of the measured effect. Two-way analysis of variance was used only where indicated.

Airyscan confocal images of endogenous GLUT4 and SEC16A colocalization were collected on a laser scanning microscope (LSM880; ZEISS) with Airyscan using a 63× objective. All other confocal images were collected on a laser scanning confocal microscope using a 63×, 1.4 NA Plan-Apochromat objective.

Western blots and antibodies

Western blot experiments were performed using standard protocols. Cellular protein extracts were collected from 3T3-L1 differentiated adipocytes expressing indicated siRNA or DNA constructs. Antibodies used were as follows: RAB10 (4262S; Cell Signaling Technology); AS160 (07–741; EMD Millipore); ACTIN (AAN01-A; Cytoskeleton, Inc.); AKT (9272S; Cell Signaling Technology); P-AKT (9271S; Cell Signaling Technology); P-AS160 (8881S; Cell Signaling Technology);

TR (ab84036; Abcam); IRAP (6918P; Cell Signaling Technology); GFP (Roche); and SEC16A (MKA0310; Cosmo Bio Co.).

RAB10 purification

Rab10 was cloned using BamHI and XhoI into pGEX-6P-1 plasmid (Promega) with a C-terminal hexa-his tag, GST-Rab10-His. GST-tagged Rab10-His protein was expressed in *Escherichia coli* BL21 (DE3) cells (Invitrogen) during overnight induction at 18°C. Bacterial pellets were resuspended in 20 mM Hepes, pH 7.2, 100 mM KCl, 1 mM TCEP, and 0.1% IGEPAL supplemented with an antiprotease cocktail (Roche) and 1 mM phenylmethylsulfonyl fluoride. The resuspended cell pellets were lysed on ice by sonication followed by ultracentrifugation at 100,000 *g* for 1 h. Fusion protein was purified by GST affinity chromatography. The N-terminal GST tag was removed by digestion with PreScission protease (Invitrogen), and Rab10-His was separated from GST and uncleaved fusion protein on glutathione-agarose. After overnight dialysis in 20 mM Hepes, pH 7.2, 100 mM KCl, and 1 mM DTT, Rab10-His was further purified using a size exclusion chromatography using Superdex200 column (GE Healthcare) in 20 mM Hepes, pH 7.2, 100 mM KCl, and 1 mM DTT. Purified protein was stored at −80°C.

GTPγS loading and column preparation for RAB10

Purified Rab10-His was loaded with GTPγS by incubation with nucleotide exchange buffer (20 mM Hepes, pH 7.5, 100 mM KCl, 5 mM MgCl$_2$, and 1 mM DTT) containing 1 mM GTPγS for 1 h at room temperature under constant agitation. After loading, GTPγS-Rab10-His was incubated with equilibrated Ni-NTA beads at 25°C for 1 h under constant agitation. After incubation, GTPγS-Rab10-His bound to beads was washed three times in wash buffer (20 mM Hepes, pH 7.5, 100 mM KCl, 20 mM imidazole, and 1 mM DTT).

Isolation of Rab10 effectors using affinity purification

3T3-L1 adipocytes were incubated with serum-free media for 2 h and then stimulated with 1 nM insulin for 30 min. Cells were lysed in RIPA buffer (50 mM Tris, pH 8.0, 150 mM NaCl, 0.5% sodium deoxycholate, 1% NP-40, and 0.1% SDS). GTPγS-Rab10-His beads were incubated with insulin-stimulated 3T3-L1 adipocyte cytosol at 4°C for 1 h under constant agitation. After incubation with cytosol, the GTPγS-Rab10-His beads and cytosol were passed through a column. The GTPγS-Rab10-His column was washed in 10 column volumes of wash buffer (20 mM Hepes, pH 7.5, 100 mM KCl, 20 mM imidazole, and 1 mM DTT) to remove nonspecific binding. GTPγS-Rab10-His and interacting proteins were eluted using three column volumes of elution buffer (20 mM Hepes, pH 7.5, 100 mM KCl, 0.5 M imidazole, and 1 mM DTT). GTPγS-Rab10-His fractions were examined by SDS-PAGE and subsequently sent for mass spectrometry.

ER secretion assay

3T3-L1 adipocytes were incubated at 37°C with 5 µg/ml Brefeldin A for 45 min to block ER exit. Cells were washed and reincubated in serum-free media without Brefeldin. The media (secreted proteins) was collected and cells solubilized after 45, 60, 120, and 180 min of recovery. The amount of adipsin in the media and associated with cells was determined by quantitative Western blotting. To calculate the rate of secretion of adipsin from cells, the amount in the media at each time point was normalized to the cell associated adipsin at the start of the incubation in Brefeldin-free media.

PLA

3T3-L1 adipocytes were electroporated with 45 µg of each indicated plasmid. Cells were incubated in serum free media for 2 h and then stimulated with 1 nM insulin for 30 min where indicated. Cells were

washed three times with PBS before fixation for 7–10 min in 3.7% formaldehyde. Cells were permeabilized with 0.25 mg/ml saponin and immunostained with mouse anti-FLAG antibody (F7425; Abcam) and rabbit anti-GFP antibody (ab6556; Abcam) for 30 min, after which PLA was performed according to the instructions of the manufacturer (Duolink In Situ Orange Starter kit Mouse/Rabbit; Sigma-Aldrich). For quantification, signals in at least 30 cell images were quantified in each experiment, for three experiments. Images are representative of the results of three independent experiments.

GLUT4 exocytosis assay

3T3-L1 adipocytes electroporated with HA-GLUT4-GFP and indicated siRNA were serum starved for 2 h and incubated with 1 nM insulin for 1 h. Cells were then incubated with anti-HA antibodies (100 µg/ml) in the presence of 1nM insulin for 5, 10, 15, 30, 45, and 60 min. Cells were fixed with 3.7% formaldehyde for 7–10 min, permeabilized with 0.25 mg/ml saponin, and then stained with anti–mouse Cy3 to label the entire pool of antibody-labeled HA-GLUT4-GFP. Cells were imaged and the Cy3-to-GFP (total GLUT4) ratio was determined over time. The rate of exocytosis was determined by measuring the slope of the curve.

TIRF microscopy assays

For TIRF microscopy experiments, dual-color TIRF and epifluorescence images were acquired on a Nikon TiE inverted microscope with perfect focus mechanism using a 63×, 1.49 NA objective and Neo sCMOS camera (Andor Technology). Excitation wavelengths at 488 for GFP and 561 for Cy3 were used.

3T3-L1 adipocytes were electroporated with 45 µg of HA-GLUT4-GFP. Cells were incubated in serum-free media for 2 h and then stimulated with 1 nM insulin for 30 min where indicated. Cells were fixed for 7–10 min in 3.7% formaldehyde, permeabilized with 0.25 mg/ml saponin, and immunostained with anti–mouse SEC16A antibody (MKA0310; Cosmo Bio Co.). SEC16A staining was visualized with a Cy3-tagged secondary antibody.

The Pearson's correlation coefficient (r) for HA-GLUT4-GFP and SEC16A puncta in the TIRF zone was calculated using MetaMorph image processing software by generating binary masks of GLUT4 (GFP) TIRF puncta above a fixed threshold and SEC16A (Cy3) TIRF puncta above a fixed threshold.

To calculate the SEC16A TIRF/epifluorescence ratio, the integrated anti-SEC16A (Cy3) fluorescence signal in TIRF was calculated, background corrected, and normalized to the total anti-SEC16A (Cy3) signal in epifluorescence that was also background corrected. ImageJ software was used for image quantification.

For quantification of the number of SEC16A-positive puncta in TIRF microscopy, binary masks of SEC16A TIRF puncta above a fixed threshold were generated. A size threshold was applied to only include puncta with an area >2 × 2 pixels in the analysis, and the number of puncta were counted using ImageJ software.

IRAP-TR mobilization from the perinuclear regions assay

3T3-L1 adipocytes electroporated with IRAP-TR, and indicated siRNA were treated overnight with an antibody against mouse TR to block endogenous TR expression. The next day, cells were incubated in serum free DMEM containing 1 nM insulin and 5 µg/ml Tf-Alexa[488] or Tf-Cy3 for 1 h to label the entire pool of IRAP-TR. They were then washed three times in PBS and incubated in serum-free DMEM containing 1 nM insulin and 8 µg/ml unlabeled Tf for indicated time points. Cells were fixed with 3.7% formaldehyde for 7–10 min, permeabilized with 0.25 mg/ml saponin, and then stained with an antibody against human to label the total IRAP-TR pool. Staining was visualized with fluorescently tagged secondary antibodies. A mask was generated by creating a circle of fixed size that tightly encircled both the nucleus and those pixels that colocalized with perinuclear HA-GLUT4-GFP. This circle was drawn around the nucleus of IRAP-TR–expressing cells such that it encircled both the nucleus and perinuclear regions, allowing us to restrict our analysis to this region. The total Tf-Cy3/Alexa[488] signal within this restricted region was measured and ratioed to the amount of total IRAP-TR expression in this region. The decrease in this ratio over time is indicative of IRAP-TR mobilization from this perinuclear region. Each siRNA treatment was normalized to its starting ratio to control for differences in Tf-Cy3/Alexa[488] uptake. These ratios were then plotted, and the data were fit to an exponential decay curve.

Immunoabsorption of native GLUT4-containing compartments

3T3-L1 adipocytes that stably express HA-GLUT4-GFP were electroporated with or without 4 nmol SEC16A siRNA, as indicated. Cells were washed and incubated in media without sera for 2 h. Cells were then stimulated with or without 1 nM insulin for 30 min to achieve steady-state surface GLUT4 levels. Cells were lysed in cold HES buffer (20 mM Hepes, 1 mM EDTA, 250 mM sucrose, and protease inhibitors) using a cell scraper on ice. They were homogenized by subsequent passaging through 23G and 27G 1 1/4 syringes on ice. Lysates were spun at 700 g for 10 min at 4°C. Supernatant was collected and incubated for 30 min at 4°C with µMACS anti-GFP MicroBeads (Miltenyi Biotec). In different experiments as noted, different amounts of microbeads were used to vary the efficiency of immunoabsorption of GLUT4-containing membranes. The sample was loaded onto a MACS column (Miltenyi Biotec) and placed in the magnetic field of a µMACS Separator in which the magnetically labeled HA-GLUT4-GFP–containing compartments were retained. Columns were washed with PBS and eluted with denaturing elution buffer (50 mM Tris HCl, pH 6.08, 50 mM DTT, 1% SDS, 1 nM EDTA, 0.005% bromphenol blue, and 10% glycerol). Western blots were performed on lysates, flow through, and elution fractions, probing for the indicated proteins. Band intensity was quantified using ImageJ and normalized to the amount of GFP eluted in each sample to control for immunoabsorption efficiency. Amounts of indicated proteins in the elution fraction were normalized to the amount of that protein in the control sample.

Online supplemental material

Fig. S1 shows RT-PCR quantification of SEC16A, IQGAP1, ARH GEF7, GIT1, PFN1, ANXA2, SEC13, LRRK2, SEC23A, SEC23B, and SEC31 knockdown. Fig. S2 shows adipsin secretion is blunted by SEC16A and SEC13 knockdown, but not by SEC23A or RAB10 knockdown. Fig. S3 shows SEC16A encircles perinuclear GLUT4 in adipocytes. Fig. S4 shows the ER marker Sec61B-GFP does not colocalize with perinuclear SEC16A or encircle perinuclear GLUT4. Fig. S5 shows SEC16A knockdown does not alter RAB10 or AS160 expression. Online supplemental material is available at http://www.jcb.org/cgi/content/full/jcb.201509052/DC1. Additional data are available in the JCB DataViewer at http://dx.doi.org/10.1083/jcb.201509052.dv.

References

Abel, E.D., O. Peroni, J.K. Kim, Y.B. Kim, O. Boss, E. Hadro, T. Minnemann, G.I. Shulman, and B.B. Kahn. 2001. Adipose-selective targeting of the GLUT4 gene impairs insulin action in muscle and liver. *Nature.* 409:729–733. http://dx.doi.org/10.1038/35055575

Babbey, C.M., N. Ahktar, E. Wang, C.C. Chen, B.D. Grant, and K.W. Dunn. 2006. Rab10 regulates membrane transport through early endosomes of polarized Madin-Darby canine kidney cells. *Mol. Biol. Cell.* 17:3156–3175. http://dx.doi.org/10.1091/mbc.E05-08-0799

Babbey, C.M., R.L. Bacallao, and K.W. Dunn. 2010. Rab10 associates with primary cilia and the exocyst complex in renal epithelial cells. *Am. J. Physiol. Renal Physiol.* 299:F495–F506. http://dx.doi.org/10.1152/ajprenal.00198.2010

Bai, L., Y. Wang, J. Fan, Y. Chen, W. Ji, A. Qu, P. Xu, D.E. James, and T. Xu. 2007. Dissecting multiple steps of GLUT4 trafficking and identifying the sites of insulin action. *Cell Metab.* 5:47–57. http://dx.doi.org/10.1016/j.cmet.2006.11.013

Bhattacharyya, D., and B.S. Glick. 2007. Two mammalian Sec16 homologues have nonredundant functions in endoplasmic reticulum (ER) export and transitional ER organization. *Mol. Biol. Cell.* 18:839–849. http://dx.doi.org/10.1091/mbc.E06-08-0707

Budnik, A., and D.J. Stephens. 2009. ER exit sites--localization and control of COPII vesicle formation. *FEBS Lett.* 583:3796–3803. http://dx.doi.org/10.1016/j.febslet.2009.10.038

Chen, S., D.H. Wasserman, C. MacKintosh, and K. Sakamoto. 2011. Mice with AS160/TBC1D4-Thr649Ala knockin mutation are glucose intolerant with reduced insulin sensitivity and altered GLUT4 trafficking. *Cell Metab.* 13:68–79. http://dx.doi.org/10.1016/j.cmet.2010.12.005

Chen, Y., Y. Wang, J. Zhang, Y. Deng, L. Jiang, E. Song, X.S. Wu, J.A. Hammer, T. Xu, and J. Lippincott-Schwartz. 2012. Rab10 and myosin-Va mediate insulin-stimulated GLUT4 storage vesicle translocation in adipocytes. *J. Cell Biol.* 198:545–560. http://dx.doi.org/10.1083/jcb.201111091

Cho, H.J., J. Yu, C. Xie, P. Rudrabhatla, X. Chen, J. Wu, L. Parisiadou, G. Liu, L. Sun, B. Ma, et al. 2014. Leucine-rich repeat kinase 2 regulates Sec16A at ER exit sites to allow ER-Golgi export. *EMBO J.* 33:2314–2331. http://dx.doi.org/10.15252/embj.201487807

Connerly, P.L., M. Esaki, E.A. Montegna, D.E. Strongin, S. Levi, J. Soderholm, and B.S. Glick. 2005. Sec16 is a determinant of transitional ER organization. *Curr. Biol.* 15:1439–1447. http://dx.doi.org/10.1016/j.cub.2005.06.065

D'Arcangelo, J.G., K.R. Stahmer, and E.A. Miller. 2013. Vesicle-mediated export from the ER: COPII coat function and regulation. *Biochim. Biophys. Acta.* 1833:2464–2472. http://dx.doi.org/10.1016/j.bbamcr.2013.02.003

Deen, A.J., K. Rilla, S. Oikari, R. Kärnä, G. Bart, J. Häyrinen, A.R. Bathina, A. Ropponen, K. Makkonen, R.H. Tammi, and M.I. Tammi. 2014. Rab10-mediated endocytosis of the hyaluronan synthase HAS3 regulates hyaluronan synthesis and cell adhesion to collagen. *J. Biol. Chem.* 289:8375–8389. http://dx.doi.org/10.1074/jbc.M114.552133

Eguez, L., A. Lee, J.A. Chavez, C.P. Miinea, S. Kane, G.E. Lienhard, and T.E. McGraw. 2005. Full intracellular retention of GLUT4 requires

AS160 Rab GTPase activating protein. *Cell Metab.* 2:263–272. http://dx.doi.org/10.1016/j.cmet.2005.09.005

English, A.R., and G.K. Voeltz. 2013. Rab10 GTPase regulates ER dynamics and morphology. *Nat. Cell Biol.* 15:169–178. http://dx.doi.org/10.1038/ncb2647

Foley, K.P., and A. Klip. 2014. Dynamic GLUT4 sorting through a syntaxin-6 compartment in muscle cells is derailed by insulin resistance-causing ceramide. *Biol. Open.* 3:314–325. http://dx.doi.org/10.1242/bio.20147898

Friedman, J.R., B.M. Webster, D.N. Mastronarde, K.J. Verhey, and G.K. Voeltz. 2010. ER sliding dynamics and ER-mitochondrial contacts occur on acetylated microtubules. *J. Cell Biol.* 190:363–375. http://dx.doi.org/10.1083/jcb.200911024

Giordano, F., Y. Saheki, O. Idevall-Hagren, S.F. Colombo, M. Pirruccello, I. Milosevic, E.O. Gracheva, S.N. Bagriantsev, N. Borgese, and P. De Camilli. 2013. PI(4,5)P(2)-dependent and Ca(2+)-regulated ER-PM interactions mediated by the extended synaptotagmins. *Cell.* 153:1494–1509. http://dx.doi.org/10.1016/j.cell.2013.05.026

Gonzalez, E., and T.E. McGraw. 2006. Insulin signaling diverges into Akt-dependent and -independent signals to regulate the recruitment/docking and the fusion of GLUT4 vesicles to the plasma membrane. *Mol. Biol. Cell.* 17:4484–4493. http://dx.doi.org/10.1091/mbc.E06-07-0585

Habraken, J.B., J. Booij, P. Slomka, E.B. Sokole, and E.A. van Royen. 1999. Quantification and visualization of defects of the functional dopaminergic system using an automatic algorithm. *J. Nucl. Med.* 40:1091–1097.

Huang, S., and M.P. Czech. 2007. The GLUT4 glucose transporter. *Cell Metab.* 5:237–252. http://dx.doi.org/10.1016/j.cmet.2007.03.006

Huang, G., D. Buckler-Pena, T. Nauta, M. Singh, A. Asmar, J. Shi, J.Y. Kim, and K.V. Kandror. 2013. Insulin responsiveness of glucose transporter 4 in 3T3-L1 cells depends on the presence of sortilin. *Mol. Biol. Cell.* 24:3115–3122. http://dx.doi.org/10.1091/mbc.E12-10-0765

Hughes, H., A. Budnik, K. Schmidt, K.J. Palmer, J. Mantell, C. Noakes, A. Johnson, D.A. Carter, P. Verkade, P. Watson, and D.J. Stephens. 2009. Organisation of human ER-exit sites: requirements for the localisation of Sec16 to transitional ER. *J. Cell Sci.* 122:2924–2934. http://dx.doi.org/10.1242/jcs.044032

Iinuma, T., A. Shiga, K. Nakamoto, M.B. O'Brien, M. Aridor, N. Arimitsu, M. Tagaya, and K. Tani. 2007. Mammalian Sec16/p250 plays a role in membrane traffic from the endoplasmic reticulum. *J. Biol. Chem.* 282:17632–17639. http://dx.doi.org/10.1074/jbc.M611237200

Jedrychowski, M.P., C.A. Gartner, S.P. Gygi, L. Zhou, J. Herz, K.V. Kandror, and P.F. Pilch. 2010. Proteomic analysis of GLUT4 storage vesicles reveals LRP1 to be an important vesicle component and target of insulin signaling. *J. Biol. Chem.* 285:104–114. http://dx.doi.org/10.1074/jbc.M109.040428

Jordens, I., D. Molle, W. Xiong, S.R. Keller, and T.E. McGraw. 2010. Insulin-regulated aminopeptidase is a key regulator of GLUT4 trafficking by controlling the sorting of GLUT4 from endosomes to specialized insulin-regulated vesicles. *Mol. Biol. Cell.* 21:2034–2044. http://dx.doi.org/10.1091/mbc.E10-02-0158

Karunanithi, S., T. Xiong, M. Uhm, D. Leto, J. Sun, X.W. Chen, and A.R. Saltiel. 2014. A Rab10:RalA G protein cascade regulates insulin-stimulated glucose uptake in adipocytes. *Mol. Biol. Cell.* 25:3059–3069. http://dx.doi.org/10.1091/mbc.E14-06-1060

Karylowski, O., A. Zeigerer, A. Cohen, and T.E. McGraw. 2004. GLUT4 is retained by an intracellular cycle of vesicle formation and fusion with endosomes. *Mol. Biol. Cell.* 15:870–882. http://dx.doi.org/10.1091/mbc.E03-07-0517

Kasprzak, J.D., W.B. Vletter, J.R. Roelandt, J.R. van Meegen, R. Johnson, and F.J. Ten Cate. 1998. Visualization and quantification of myocardial mass at risk using three-dimensional contrast echocardiography. *Cardiovasc. Res.* 40:314–321. http://dx.doi.org/10.1016/S0008-6363(98)00178-3

Khoriaty, R., M.P. Vasievich, and D. Ginsburg. 2012. The COPII pathway and hematologic disease. *Blood.* 120:31–38. http://dx.doi.org/10.1182/blood-2012-01-292086

Lampson, M.A., A. Racz, S.W. Cushman, and T.E. McGraw. 2000. Demonstration of insulin-responsive trafficking of GLUT4 and vpTR in fibroblasts. *J. Cell Sci.* 113:4065–4076.

Lampson, M.A., J. Schmoranzer, A. Zeigerer, S.M. Simon, and T.E. McGraw. 2001. Insulin-regulated release from the endosomal recycling compartment is regulated by budding of specialized vesicles. *Mol. Biol. Cell.* 12:3489–3501. http://dx.doi.org/10.1091/mbc.12.11.3489

Larance, M., G. Ramm, J. Stöckli, E.M. van Dam, S. Winata, V. Wasinger, F. Simpson, M. Graham, J.R. Junutula, M. Guilhaus, and D.E. James. 2005. Characterization of the role of the Rab GTPase-activating protein AS160 in insulin-regulated GLUT4 trafficking. *J. Biol. Chem.* 280:37803–37813. http://dx.doi.org/10.1074/jbc.M503897200

Lerner, D.W., D. McCoy, A.J. Isabella, A.P. Mahowald, G.F. Gerlach, T.A. Chaudhry, and S. Horne-Badovinac. 2013. A Rab10-dependent mechanism for polarized basement membrane secretion during organ morphogenesis. *Dev. Cell.* 24:159–168. http://dx.doi.org/10.1016/j.devcel.2012.12.005

Leto, D., and A.R. Saltiel. 2012. Regulation of glucose transport by insulin: traffic control of GLUT4. *Nat. Rev. Mol. Cell Biol.* 13:383–396. http://dx.doi.org/10.1038/nrm3351

Lizunov, V.A., J.P. Lee, M.C. Skarulis, J. Zimmerberg, S.W. Cushman, and K.G. Stenkula. 2013. Impaired tethering and fusion of GLUT4 vesicles in insulin-resistant human adipose cells. *Diabetes.* 62:3114–3119. http://dx.doi.org/10.2337/db12-1741

Martin, O.J., A. Lee, and T.E. McGraw. 2006. GLUT4 distribution between the plasma membrane and the intracellular compartments is maintained by an insulin-modulated bipartite dynamic mechanism. *J. Biol. Chem.* 281:484–490. http://dx.doi.org/10.1074/jbc.M505944200

Martin, S., C.A. Millar, C.T. Lyttle, T. Meerloo, B.J. Marsh, G.W. Gould, and D.E. James. 2000a. Effects of insulin on intracellular GLUT4 vesicles in adipocytes: evidence for a secretory mode of regulation. *J. Cell Sci.* 113:3427–3438.

Martin, S., G. Ramm, C.T. Lyttle, T. Meerloo, W. Stoorvogel, and D.E. James. 2000b. Biogenesis of insulin-responsive GLUT4 vesicles is independent of brefeldin A-sensitive trafficking. *Traffic.* 1:652–660. http://dx.doi.org/10.1034/j.1600-0854.2000.010809.x

Millar, C.A., T. Meerloo, S. Martin, G.R. Hickson, N.J. Shimwell, M.J. Wakelam, D.E. James, and G.W. Gould. 2000. Adipsin and the glucose transporter GLUT4 traffic to the cell surface via independent pathways in adipocytes. *Traffic.* 1:141–151. http://dx.doi.org/10.1034/j.1600-0854.2000.010206.x

Miller, E.A., and C. Barlowe. 2010. Regulation of coat assembly--sorting things out at the ER. *Curr. Opin. Cell Biol.* 22:447–453. http://dx.doi.org/10.1016/j.ceb.2010.04.003

Penn, M.S., M.R. Koelle, S.M. Schwartz, and G.M. Chisolm. 1990. Visualization and quantification of transmural concentration profiles of macromolecules across the arterial wall. *Circ. Res.* 67:11–22. http://dx.doi.org/10.1161/01.RES.67.1.11

Perera, H.K., M. Clarke, N.J. Morris, W. Hong, L.H. Chamberlain, and G.W. Gould. 2003. Syntaxin 6 regulates Glut4 trafficking in 3T3-L1 adipocytes. *Mol. Biol. Cell.* 14:2946–2958. http://dx.doi.org/10.1091/mbc.E02-11-0722

Rowland, A.A., P.J. Chitwood, M.J. Phillips, and G.K. Voeltz. 2014. ER contact sites define the position and timing of endosome fission. *Cell.* 159:1027–1041. http://dx.doi.org/10.1016/j.cell.2014.10.023

Sadacca, L.A., J. Bruno, J. Wen, W. Xiong, and T.E. McGraw. 2013. Specialized sorting of GLUT4 and its recruitment to the cell surface are independently regulated by distinct Rabs. *Mol. Biol. Cell.* 24:2544–2557. http://dx.doi.org/10.1091/mbc.E13-02-0103

Sano, H., S. Kane, E. Sano, C.P. Mîinea, J.M. Asara, W.S. Lane, C.W. Garner, and G.E. Lienhard. 2003. Insulin-stimulated phosphorylation of a Rab GTPase-activating protein regulates GLUT4 translocation. *J. Biol. Chem.* 278:14599–14602. http://dx.doi.org/10.1074/jbc.C300063200

Sano, H., L. Eguez, M.N. Teruel, M. Fukuda, T.D. Chuang, J.A. Chavez, G.E. Lienhard, and T.E. McGraw. 2007. Rab10, a target of the AS160 Rab GAP, is required for insulin-stimulated translocation of GLUT4 to the adipocyte plasma membrane. *Cell Metab.* 5:293–303. http://dx.doi.org/10.1016/j.cmet.2007.03.001

Sano, H., G.R. Peck, S. Blachon, and G.E. Lienhard. 2015. A potential link between insulin signaling and GLUT4 translocation: Association of Rab10-GTP with the exocyst subunit Exoc6/6b. *Biochem. Biophys. Res. Commun.* 465:601–605. http://dx.doi.org/10.1016/j.bbrc.2015.08.069

Shewan, A.M., E.M. van Dam, S. Martin, T.B. Luen, W. Hong, N.J. Bryant, and D.E. James. 2003. GLUT4 recycles via a trans-Golgi network (TGN) subdomain enriched in Syntaxins 6 and 16 but not TGN38: involvement of an acidic targeting motif. *Mol. Biol. Cell.* 14:973–986. http://dx.doi.org/10.1091/mbc.E02-06-0315

Shi, J., and K.V. Kandror. 2005. Sortilin is essential and sufficient for the formation of Glut4 storage vesicles in 3T3-L1 adipocytes. *Dev. Cell.* 9:99–108. http://dx.doi.org/10.1016/j.devcel.2005.04.004

Söderberg, O., M. Gullberg, M. Jarvius, K. Ridderstråle, K.J. Leuchowius, J. Jarvius, K. Wester, P. Hydbring, F. Bahram, L.G. Larsson, and U. Landegren. 2006. Direct observation of individual endogenous protein complexes in situ by proximity ligation. *Nat. Methods.* 3:995–1000. http://dx.doi.org/10.1038/nmeth947

Sprangers, J., and C. Rabouille. 2015. SEC16 in COPII coat dynamics at ER exit sites. *Biochem. Soc. Trans.* 43:97–103. http://dx.doi.org/10.1042/BST20140283

Stöckli, J., D.J. Fazakerley, and D.E. James. 2011. GLUT4 exocytosis. *J. Cell Sci.* 124:4147–4159. http://dx.doi.org/10.1242/jcs.097063

Subtil, A., M.A. Lampson, S.R. Keller, and T.E. McGraw. 2000. Characterization of the insulin-regulated endocytic recycling mechanism in 3T3-L1 adipocytes using a novel reporter molecule. *J. Biol. Chem.* 275:4787–4795. http://dx.doi.org/10.1074/jbc.275.7.4787

Tillmann, K.D., V. Reiterer, F. Baschieri, J. Hoffmann, V. Millarte, M.A. Hauser, A. Mazza, N. Atias, D.F. Legler, R. Sharan, et al. 2015. Regulation of Sec16 levels and dynamics links proliferation and secretion. *J. Cell Sci.* 128:670–682. http://dx.doi.org/10.1242/jcs.157115

Vazirani, R.P., A. Verma, L.A. Sadacca, M.S. Buckman, B. Picatoste, M. Beg, C. Torsitano, J.H. Bruno, R.T. Patel, K. Simonyte, et al. 2016. Disruption of adipose Rab10-dependent insulin signaling causes hepatic insulin resistance. *Diabetes.* 65:1577–1589. http://dx.doi.org/10.2337/db15-1128

Watson, P., A.K. Townley, P. Koka, K.J. Palmer, and D.J. Stephens. 2006. Sec16 defines endoplasmic reticulum exit sites and is required for secretory cargo export in mammalian cells. *Traffic.* 7:1678–1687. http://dx.doi.org/10.1111/j.1600-0854.2006.00493.x

Whittle, J.R., and T.U. Schwartz. 2010. Structure of the Sec13-Sec16 edge element, a template for assembly of the COPII vesicle coat. *J. Cell Biol.* 190:347–361. http://dx.doi.org/10.1083/jcb.201003092

Xiong, W., I. Jordens, E. Gonzalez, and T.E. McGraw. 2010. GLUT4 is sorted to vesicles whose accumulation beneath and insertion into the plasma membrane are differentially regulated by insulin and selectively affected by insulin resistance. *Mol. Biol. Cell.* 21:1375–1386. http://dx.doi.org/10.1091/mbc.E09-08-0751

Xu, X.H., C.Y. Deng, Y. Liu, M. He, J. Peng, T. Wang, L. Yuan, Z.S. Zheng, P.J. Blackshear, and Z.G. Luo. 2014. MARCKS regulates membrane targeting of Rab10 vesicles to promote axon development. *Cell Res.* 24:576–594. http://dx.doi.org/10.1038/cr.2014.33

Zeigerer, A., M.A. Lampson, O. Karylowski, D.D. Sabatini, M. Adesnik, M. Ren, and T.E. McGraw. 2002. GLUT4 retention in adipocytes requires two intracellular insulin-regulated transport steps. *Mol. Biol. Cell.* 13:2421–2435. http://dx.doi.org/10.1091/mbc.E02-02-0071